Periodica Polytechnica
Civil Engineering

60(4), pp. 619–645, 2016
DOI: 10.3311/PPci.8728


RESEARCH ARTICLE

# A Comparison of Large Deflection Analysis of Bending Plates by Dynamic Relaxation

*Mohammad* Rezaiee-Pajand, *Hossein* Estiri

Received 29-10-2015, revised 31-01-2016, accepted 02-02-2016

***Abstract***

*In this paper, various dynamic relaxation methods are investigated for geometric nonlinear analysis of bending plates. Sixteen wellknown algorithms are employed. Dynamic relaxation fictitious parameters are the mass matrix, the damping matrix and the time step. The difference between the mentioned tactics is how to implement these parameters. To compare the efficiency of these strategies, several bending plates' problems with large deflections are solved. Based on the number of iterations and analysis time, the scores of the different schemes are calculated. These scores determine the ranking of each technique. The numerical results indicate the appropriate efficiency of Underwood and Rezaiee-Pajand & Alamatian processes for the nonlinear analysis of bending plates.*

***Keywords***

*Dynamic relaxation · Mass · Damping · Time step · Large deformations · Bending plate*

**Mohammad Rezaiee-Pajand**
Civil Engineering Department, Ferdowsi University of Mashhad, Mashhad, Vakilabad Highway, 9177948974, Iran
e-mail: rezaiee@um.ac.ir

**Hossein Estiri**
Civil Engineering Department, Ferdowsi University of Mashhad, Mashhad, Vakilabad Highway, 9177948974, Iran

## 1 Introduction

Bending plate structures are important in mechanical and civil engineering. Therefore, a great deal of research has been done to describe their behavior [1]. Von Kármán formulated differential equations for large deformations of plates in 1910. Levy solved Von Kármán's equations using trigonometric functions and Fourier series. He obtained the equations that govern the behavior of quadrilateral thin plate bending with large displacements [2]. Bergan and Clough established finite element models for thin plates and shells based on Rayleigh-Ritz method [3]. Yang and Bhatti formulated a nonlinear element for solving the static and dynamic cases of plate bending by using the updated Lagrangian approach [4].

The analysis of elastic plates with large deformations is very difficult and there are few approaches to find an exact solution. Numerical and approximate solution procedures were developed for large displacements with the increasing processing power of modern computers. One of these tactics is called dynamic relaxation. Rushton is the first one to apply this scheme to find the solution of nonlinear problems [5]. Moreover, this investigator employed dynamic relaxation technique to analyze stress and post-buckling behavior of plates [6]. Taking into account the geometric nonlinearity, the following equations describing the state of plate movements were used in the mentioned reference:

$$u = u_0 - z\frac{\partial w}{\partial x},\quad v = v_0 - z\frac{\partial w}{\partial y},\quad w = w_0 \tag{1}$$

In these relations, $u_0$, $v_0$ and $w_0$ are the mid-plane displacements in the x, y and z-direction, respectively. The nonlinear stiffness formulations for large deflection analysis of plates are utilized for the rectangular plate finite element. The elements have five degrees of freedom at each nodal point. Two of these are in-plane displacements, u and v in the x and y directions, correspondingly. One transverse deflection w; two rotations $w_x$, and $w_y$, about the y and x axes, respectively, are the other three degrees of freedom. In this structure, the normal strains in the x, y directions are $\varepsilon_x$ and $\varepsilon_y$, correspondingly. Moreover,$\gamma_{xy}$shows the shear strain. The plate strains can be written in terms of the middle surface deflections, in the subsequent form:

$$\varepsilon_x = \frac{\partial u}{\partial x} + \frac{1}{2}\left(\frac{\partial w}{\partial x}\right)^2 - z\frac{\partial^2 w}{\partial x^2} \quad (2)$$

$$\varepsilon_y = \frac{\partial v}{\partial y} + \frac{1}{2}\left(\frac{\partial w}{\partial y}\right)^2 - z\frac{\partial^2 w}{\partial y^2} \quad (3)$$

$$\gamma_{xy} = \frac{\partial u}{\partial y} + \frac{\partial v}{\partial x} + \frac{\partial w}{\partial x}.\frac{\partial w}{\partial y} + 2z\frac{\partial^2 w}{\partial x \partial y} \quad (4)$$

What come in the rest of paper has been carried out on bending plate based on the dynamic relaxation scheme. Basu and Dawson used dynamic relaxation method to study the small deflection behavior of rectangular orthotropic and isotropic sandwich plates with uniform or varying cross section [7]. Rushton evaluated the buckling behavior of initially curved plates subjected to lateral loading [8]. Turvey and Wittrick analyzed the post-buckling behavior of laminated plates with large deformations [9]. Alwar and Rao proposed the nonlinear solution of orthotropic clamped plates with constant thickness and subjected to uniform lateral loading [10, 11]. Rushton and Hook obtained the response of plates and beams with large displacements and nonlinear stress and strain behavior [12]. They also carried out buckling analysis of beams and plates onto an intermediate support [13]. Frieze carried out the analysis of plates, including both the nonlinear effects of material and geometry [14]. Turvey investigated the dynamic relaxation solution in the geometric nonlinear behavior of tapered annular plates [15]. Pica carried out transient and pseudo-transient analysis of the Mindlin plates [16].

Al-Shawi and Mardirosian used a combination of finite element and dynamic relaxation method along with weighted coefficients for mass and damping to find the response of bending plates [17]. Zhang and Yu proposed an improved adaptive dynamic relaxation algorithm and used it to solve the elasto-plastic bending of circular plates [18]. Turvey and Osman utilized finite difference dynamic relaxation strategy to geometrically nonlinear analysis of isotropic rectangular Mindlin plates [19]. Turvey and Salehi analyzed the large deformation of sector plates subject to uniform loading by using the dynamic relaxation and finite difference methods [20]. They made comparison studies, as well [21]. Kadkhodyan and Zhang carried out buckling and post-buckling analysis of plates using dynamic stability criteria and the dynamic relaxation process [22]. Turvey and Salehi studied linear and nonlinear analysis of the composite plates [23]. Salehi and Aghaei investigated circular viscoelastic plates. They applied the effect of higher-order shear deformations in their formulation [24]. Falahatgar and Salehi carried out a post-buckling analysis of the annular sector plate. They also evaluated geometrically nonlinear analysis of polymeric plates. They analyzed higher-order shear deformations by utilizing a finite difference form of the dynamic relaxation technique [25]. Moreover, they studied geometrically nonlinear viscoelastic analysis of annular sector composite plates [26]. Golmakani and Kadkhodayan investigated the nonlinear bending of FGM annular sector plates [27]. Falahatgar and Salehi found the solution to the bending response of unidirectional polymeric laminated composite plates [28].

At this stage, a brief review of the fictitious parameters' estimation for the dynamic relaxation procedure is presented. Brew and Brotton suggested that the mass of each degree of freedom be proportional to its diagonal element in the structural stiffness matrix [29]. Bunce presented a method for calculating critical damping in the dynamic relaxation tactic using Rayleigh principle [30]. Cassel and Hobbs estimated the artificial mass by using Gershgorin's circle theorem to check the convergence and numerical stability of nonlinear analysis with the dynamic relaxation scheme [31]. Papadrakakis suggested an automatic technique for finding the fictitious parameters. The difficulty of his solution is in the first assumption of two factors [32]. Underwood presented one of the most famous formulations for dynamic relaxation iterations [33]. Qiang obtained the artificial damping and time using Rayleigh principle [34]. Zhang et al. proposed the nodal damping model [35]. Munjiza et al. supposed that damping is proportional to the power of the mass and stiffness matrices. They showed that when the damping matrix is $2M(M^{-1}S)^{0.5}$, all modes will be critically damped [36, 37].

Rezaiee-Pajand and Taghavian Hakkak calculated displacement by utilizing the first three terms of Taylor series [38]. Kadkhodayan et al. obtained a relationship for the time step by minimizing the residual forces [39]. Rezaiee-Pajand and Sarafrazi presented the optimal time step ratio and the critical damping for nonlinear structural analysis [40]. Moreover, Rezaiee-Pajand and Alamatian proposed a new approach for estimating the fictitious damping and mass [41]. In addition, Rezaiee-Pajand et al. presented a new algorithm for the calculation of the damping matrix [42]. This was reached by minimizing the error between two successive steps. Sarafrazi and Rezaiee-Pajand suggested an equation for finding the time step ratio. The damping is zero in their process [43]. Rezaiee-Pajand et al. obtained another tactic for artificial time step based on the unbalanced energy [44]. Alamatian developed a new equation to evaluate the fictitious mass in kinetic dynamic relaxation [45]. Rezaiee-Pajand et al. investigated the efficiency of twelve methods of dynamic relaxation for the finite element analysis of frame and truss structures [46]. They introduced the top five procedures by comparing their performance. Rezaiee-Pajand and Rezaiee proposed a new time step for kinetic dynamic relaxation in the latest study [47].

The available research papers indicate that many studies have been carried out about the dynamic relaxation analysis of bending plate. According to what was stated so far, there are different solution approaches for finding the large deflection in these problems. However, the effectiveness of the various dynamic relaxation schemes in the geometrically nonlinear analyses of bending plate has not been studied yet. In this paper, sixteen different known dynamic relaxation processes are studied. It should be noted that the difference between these schemes is in the estimation of the fictitious parameters. Dunkerley method is used to find the fictitious damping matrix. This approach has not been implemented so far. In order to improve the performance of the mentioned techniques, the authors also suggest some of the artificial factors for different tactics. A score will be assigned to each procedure based on the number of iterations or the total duration analysis. The final ranking of each algorithm will be obtained after solving all the problems.

## 2 The dynamic relaxation method

Dynamic relaxation is one of the explicit methods to solve a system of simultaneous equations. In this process, a fictitious mass and damping are added to the static structural equations system to obtain a fictitious dynamic system. In the dynamic relaxation approach, the velocity variations are assumed to be linear and the acceleration is supposed to be constant for each time step $t$. Thus, the following equalities can be obtained for the iterative relations of this tactic by using central finite differences:

$$\dot{X}_i^{n+\frac{1}{2}} = \frac{2m_{ii}^n - C_{ii}^n t^n}{2m_{ii}^n + C_{ii}^n t^n}\dot{X}_i^{n-\frac{1}{2}} + \frac{2t^n}{2m_{ii}^n + C_{ii}^n t^n}(p_i^n - f_i^n), \quad i = 1, 2, \dots, ndof \tag{5}$$

$$X_i^{n+1} = X_i^n + t^{n+1}\dot{X}_i^{n+\frac{1}{2}}, \quad i = 1, 2, \dots, ndof \tag{6}$$

The terms $m_{ii}^n$, $C_{ii}^n$, $t^n$ and $f_i^n$, are the *i-th* diagonal entry of the fictitious mass and damping matrices, the virtual time step, the *i-th* entry of the internal force vector in the *n-th* iteration of the dynamic relaxation procedure, respectively. The external load of the static structure is displayed with $p_i^n$. Moreover, *ndof* denotes the number of degrees of freedom for the system. Furthermore, the vectors $X$ and $\dot{X}$ indicate the displacement and velocity, correspondingly. Equalities (5) and (6) are repeated until convergence to a stable response is achieved. It is assumed that the mass and damping matrices are diagonal. This assumption leads to the explicit solutions for the relations of the dynamic relaxation scheme, and they are solved by using vector operators alone. It should be noted that the vector of residual force **R** that causes fictitious oscillations of the structure has following relation:

$$R = P - F \tag{7}$$

There are various techniques to estimate the artificial parameters. It is worth noting that the stability of dynamic relaxation solution greatly depends on the mass and the damping. Hence, extensive researches have been carried out to find these matrices. Moreover, some schemes have also been proposed for the time step. The most well-known strategies for the fictitious parameters of dynamic relaxation approach are presented in the rest of the paper.

### 2.1 Papadrakakis method

Papadrakakis proposed an automated algorithm for finding the factors needed in the dynamic relaxation scheme [32]. He assumed that the mass and damping matrices are as follows:

$$M = \rho D, \quad C = cD \tag{8}$$

Where $\rho$ and $c$ are the mass and damping factors, respectively. Moreover, **D** is a diagonal matrix whose entries are the main diagonal entries of the stiffness matrix. Papadrakakis used the following equality for estimating the optimum factors:

$$\left(\frac{t^2}{\rho}\right)_{opt} = \frac{4}{\lambda_{B\max} + \lambda_{B\min}} \tag{9}$$

$$\left(\frac{ct}{\rho}\right)_{opt} = \frac{4\sqrt{\lambda_{B\max}.\lambda_{B\min}}}{\lambda_{B\max} + \lambda_{B\min}} \tag{10}$$

In the present relation, $\lambda_{B\min}$ and $\lambda_{B\max}$ are the minimum and maximum eigenvalues for the matrix $B = D^{-1}S$, correspondingly. The stiffness matrix is shown by **S**. Lower and upper bounds can be obtained from the Eqs. (11) and (12):

$$\lambda_{B\min} = -\frac{\lambda_{DR}^2 - \beta\lambda_{DR} + \alpha}{\lambda_{DR}\gamma} \tag{11}$$

$$|\lambda_{B\max}| < \max_i \sum_{j=1}^{ndof} |b_{ij}| \tag{12}$$

The rate of error reduction between two successive iterations is shown by $\lambda_{DR}$ and can be calculated from Eq. (13) as follows:

$$\lambda_{DR} = \frac{\|X^{n+1} - X^n\|}{\|X^n - X^{n-1}\|} \tag{13}$$

Also, the factors $\alpha$, $\beta$ and $\gamma$ can be found from Eq. (14) to (16):

$$\alpha = \frac{2 - ct/\rho}{2 + ct/\rho} \tag{14}$$

$$\beta = \alpha + 1 \tag{15}$$

$$\gamma = \frac{2t^2/\rho}{2 + ct/\rho} \tag{16}$$

First, the values $\lambda_{B\min}$ and $\lambda_{B\max}$ are assigned, and the dynamic relaxation process starts. The term $\lambda_{B\min}$ is obtained from Eq. (11) when $\lambda_{DR}$ converges to a constant value. In Papadrakakis strategy, the time step is assumed to be a constant. In this paper, the time step is set to be equal 1.

### 2.2 Underwood procedure

In this method, the mass matrix is calculated using Gerschgörin circle theory. Eq. (17) shows that. Here, the symbol $S$ indicates the stiffness matrix. It is worth noting that Underwood assigned time step equal to 1.1 to ensure the stability of solution technique.

$$m_{ii} = \frac{t^2}{4} \sum_{j=1}^{ndof} \left| S_{ij} \right| \tag{17}$$

Moreover, the fictitious damping matrix is calculated from $C = 2\omega_0 M$. In this equality, $\omega_0$ is the minimum frequency of the fictitious dynamic system. This factor is estimated by using Rayleigh principle as follows.

$$\omega_0 = \sqrt{\frac{X^T S^L X}{X^T M X}} \tag{18}$$

Here, $S^L$ is the local stiffness matrix, and its elements are obtained by the following equation [33].

$$S_{ii}^{L,n} = \frac{f_i(X^n) - f_i(X^{n-1})}{t \dot{X}_i^{n-\frac{1}{2}}} \tag{19}$$

In the Eq. (18), if the value of the second root is not positive, then it is assumed that the damping is zero. The maximum value of angular frequency is two [33]. Therefore, if $\omega_0$ is greater than 2, a value less than 2 is used for it (for example, 1.9).

### 2.3 Qiang tactic

In this approach, the mass matrix is computed from the sum of the absolute values of the elements of rows of the stiffness matrix. Qiang suggested Eqs. (20) and (21) for the optimal values of damping and time step [34].

$$C_{ii} = 2\sqrt{\frac{\omega_0}{1+\omega_0}} m_{ii} \tag{20}$$

$$t = \frac{2}{\sqrt{1+\omega_0}} \tag{21}$$

Furthermore, the minimum system frequency when it is in free oscillation can be calculated as follows by using Rayleigh principle [34].

$$\omega_0 = \frac{X^T S X}{X^T M X} \tag{22}$$

### 2.4 Zhang approach

Zhang and Yu achieved the damping using Rayleigh principle as follows [18]:

$$\omega_0 = \sqrt{\frac{X^T F}{X^T M X}} \tag{23}$$

$$C = 2\omega_0 M \tag{24}$$

The fictitious mass matrix in this tactic, is like that of Underwood solution. The time step is also equal to one. It is worth emphasizing; Zhang et al. have suggested a formula for the initial displacement. In other words, these researchers used a value other than zero for the initial displacement. It should be noted that the dynamic relaxation scheme will converge to a stable response with any arbitrary initial displacement [48]. Rezaiee-Pajand et al. showed that this strategy has not a good performance for the initial displacement [46]. Hence, in this paper, zero vector is used to begin the dynamic relaxation process.

### 2.5 The nodal damping algorithm

In the previous procedures, the damping factor is the same for all degrees of freedom of the structure. Noted that this factor is calculated again in each iteration. Dynamic relaxation technique can be improved by using various damping factors. On this basis, Kadkhodayan et al. proposed the following equality to calculate the damping [35].

$$C_k = \zeta_k m_{kk} k = 1, 2, \ldots, N \tag{25}$$

$$\zeta_k^n = 2\left[\frac{(X_k^n)^T f_k^n}{(X_k^n)^T m_{kk}^n (X_k^n)}\right]^{\frac{1}{2}} \tag{26}$$

Here, the number of nodes of the structure is shown by $N$. The Eq. (26) is summed up over all the degrees of freedom at each node. The above equality shows that in this approach, the damping factor is the same for degrees of freedom of every node. The fictitious mass matrix is obtained from Eq. (17). Moreover, the time step is equal to 1.

### 2.6 Rezaiee-Pajand and Taghavian Hakkak technique

In this tactic, the diagonal elements of the mass matrix are considered to be proportional to their corresponding values in the stiffness matrix. Eq. (27) shows the mathematical formula [38]. Rezaiee-Pajand and Taghavian Hakkak proposed that $\alpha = 0.6$.

$$m_{ii} = \alpha . S_{ii} \tag{27}$$

Moreover, the damping is obtained from Qiang solution. The time step is equal to one. These researchers suggested the following equation for the displacement by using the first three polynomials of the Taylor series.

$$X^{n+1} = X^n + t\dot{X}^n + \frac{t^2}{2}\ddot{X}^n \tag{28}$$

Acceleration $\ddot{X}^n$ and velocity $\dot{X}^n$ can be obtained from equations (29) and (30), correspondingly [38].

$$R^n = M^n \ddot{X}^n + C^n \dot{X}^n \tag{29}$$

$$\dot{X}^n = \frac{X^n - X^{n-1}}{t} \tag{30}$$

## 2.7 Kinetic damping process

Dynamic relaxation is two types: viscous and kinetic. Damping is negligible in the kinetic dynamic relaxation. In other words, matrix $C$ in Eq. (5) is set to be equal to zero. When a reduction occurs in the amount of kinetic energy of the structure, it shows that a maximum point in the structural kinetic energy graph is passed. In this time, the velocity of all the degrees of freedom reset to zero. If the response at this time is used to start the next step, then convergence will not be achieved. Topping assumed that the peak of the kinetic energy occurs in the middle of the time step [49]. Thus, the displacement calculates in the middle of the step which is obtained from the following equality.

$$X_i^{n-\frac{1}{2}} = X_i^{n+1} - \frac{3}{2} t\dot{X}_i^{n+\frac{1}{2}} + \frac{t^2}{2m_{ii}} r_i^n \tag{31}$$

Thus, at the beginning of the dynamic relaxation process, displacement should be equal to (31). On the other hand, under these conditions, Eq. (5) cannot be used to calculate the speed. Hence the following equality is suggested [49].

$$\dot{X}_i^{n+\frac{1}{2}} = \frac{t}{2m_{ii}} r_i^n \tag{32}$$

Where the vector of the residual force $r_i^n$ is evaluated in the position $X_i^{n-\frac{1}{2}}$ calculated from (31). Then, the iterations of dynamic relaxation restart with these displacement and velocity vectors in order to maximize the kinetic energy again. This cycle continues until a suitable convergence is achieved. It should be noted that the fictitious time step is equal to one in this algorithm. Moreover, the mass matrix is available by Eq. (33) [50].

$$m_{ii} = \frac{t^2}{2} \sum_{j=1}^{ndof} \left|S_{ij}\right| \tag{33}$$

## 2.8 Minimum residual force method

The time step is effective in the numerical stability and convergence rate of the dynamic relaxation procedure. The dynamic behavior of structures is a time-dependent process. Hence, it needs to use a fictitious value for the time step for the transfer of the static problem to the dynamic space. This value should be obtained is such a way as to not only maintain the numerical stability of the scheme, but also reduce the number of iterations required for convergence. Kadkhodayan et al. proposed an optimum time step by minimizing the unbalanced forces [39]. Eq. (34) gives this value:

$$t^{n+1} = \frac{\sum_{i=1}^{ndof} r_i^n \dot{f}_i^{n+\frac{1}{2}}}{\sum_{i=1}^{ndof} \left(\dot{f}_i^{n+\frac{1}{2}}\right)^2} \tag{34}$$

In this relation, $\dot{f}_i^{n+\frac{1}{2}}$ is the internal force increment. The following equation shows this quantity [44].

$$\dot{f}_i^{n+\frac{1}{2}} = \sum_{j=1}^{ndof} S_{ij,T}^{\,n} \dot{X}_i^{n+\frac{1}{2}} \tag{35}$$

Here, $S_{ij,T}^{\,n}$ is a tangential stiffness matrix in the middle of the step. It is worth emphasizing; it is difficult to calculate the stiffness matrix at the middle of the step. Therefore, the values of the previous step are employed in the Eq. (35) [44]. It should be noted that the fictitious mass and damping matrices are obtained from Eqs. (17) and (24), respectively.

## 2.9 Rezaiee-Pajand and Alamatian procedure

In 2002, Rezaiee-Pajand and Alamatian presented another equality for the fictitious mass by minimizing the displacement error between two successive iterations and the linearity assumption [41].

$$m_{ii} = Max\left(\frac{(t^n)^2}{2} S_{ii}^{\,n}, \frac{(t^n)^2}{4} \sum_{j=1}^{ndof} \left|S_{ij}^{\,n}\right|\right) \tag{36}$$

Moreover, They suggested Eq. (37) to calculate the damping [41]. The fictitious minimum frequency $\omega_0$ is obtained by Eq. (23). The time step is also set equal to 1.

$$C_{ii} = \sqrt{\omega_0^2 (4 - t^2\omega_0^2)} m_{ii} \tag{37}$$

## 2.10 Minimum unbalanced energy tactic

Rezaiee-Pajand et al. wrote the out-of-balance energy function of the artificial dynamic system as follows [44]:

$$UBE = \sum_{i=1}^{ndof} \left[t^{n+1} \dot{X}_i^{n+\frac{1}{2}} \left(r_i^n - t^{n+1} \dot{f}_i^{n+\frac{1}{2}}\right)\right]^2 \tag{38}$$

They suggested another time step based on the minimal amount of Eq. (38). This proposal leads to two answers for this factor. One of these responses minimizes Eq. (38). If the characteristic equation of Eq. (38) does not have a real answer, the time step of Kadkhodayan method (Eq. (34)) will be used [44]. The mass and damping matrices are achieved from Eqs. (36) and (37), correspondingly.

## 2.11 Rezaiee-Pajand and Sarafrazi approach

In most techniques of calculating the fictitious damping, Rayleigh principle is used to obtain a minimum of eigenvalue. This principle provides an upper bound to the minimum eigenvalue [30]. Rezaiee-Pajand and Sarafrazi used the power iterative process to determine the minimum eigenvalue [40]. In each iteration of the dynamic relaxation, they used one step of the iterative power procedure. On this basis, the damping matrix is obtained from Eq. (39):

$$C_{ii}^n = \sqrt{\lambda_1^n (4 - \lambda_1^n)} m_{ii}^n \tag{39}$$

Here, $\lambda_1^n$is the transferred eigenvalue. Its value is estimated from the relation $\lambda_1^n = \lambda^n + 4$. The factor$\lambda^n$is the eigenvalue that is obtained from the iterative power algorithm. This transfer is carried out to calculate the minimum of the eigenvalue since this method yields the largest eigenvalue [46]. Moreover, this factor is compared with the minimum eigenvalue that are achieved by using Rayleigh principle, and the lower value is chosen. In this tactic, the time step is constant, and it is equal to one. Moreover, the mass is estimated by Eq. (36).

### 2.12 Zero damping technique

Rezaiee-Pajand and Sarafrazi suggested the relation between the critical damping ratio and the time step [43]. Then, they assumed the damping parameter to be zero and obtained the following formula for the time step ratio $\gamma$:

$$\gamma = \frac{t^{n+1}}{t^n} = \frac{1}{\left(1+\sqrt{\lambda_1}\right)^2} \tag{40}$$

Here, the power iteration process is used for finding the minimal eigenvalue $\lambda_1$. In this strategy, the mass matrix is provided from the Eq. (36). Furthermore, the following equation is utilized instead of Eqs. (5) and (6) in order to calculate the velocity and displacement vectors [43]:

$$\dot{X}^{n+1} = \gamma^n \left(M^{-1}R + \dot{X}^n\right) \tag{41}$$

$$X^{n+1} = X^n + \dot{X}^{n+1} \tag{42}$$

### 2.13 Dunkerley algorithm

Dunkerley method obtains a lower limit for the main frequency of oscillation [51]. In this method, the minimum frequency is obtained by Eq. (43) as follows:

$$\frac{1}{\omega_0^2} = \sum_{i=1}^{ndof} a_{ii} m_{ii} \tag{43}$$

In this relationship, $a_{ii}m_{ii}$ are the contributions of each degree of freedom when the other degrees-of freedom are absent. Hence:

$$a_{ii} m_{ii} = \frac{1}{\omega_{ii}^2} \tag{44}$$

The symbol $\omega_{ii}$ is the system frequency with a single degree of freedom with mass $m_{ii}$, for the ***i-th*** degree of freedom. On this basis, Dunkerley relationship is as follows:

$$\frac{1}{\omega_0^2} = \sum_{i=1}^{ndof} \frac{1}{\omega_{ii}^2} \tag{45}$$

The calculation of the mass and damping matrices is performed by Eqs. (36) and (37). Moreover, the applied time step is equal to 1.

## 3 Numerical examples

All the methods presented in the previous section were programmed in the FORTRAN language. The geometrically nonlinear analysis of various plates was carried out using this program. The loads were entered into ten increments, and then the answers were obtained. The number of iterations and analysis time for each structure are listed in the tables. The load-displacement curves are plotted. The accuracy is the same for these approaches. However, each tactic requires a different number of iterations to achieve the desired accuracy. The steps in the dynamic relaxation process for the analysis of structures are as follows:

*Step 1* - Choose the initial velocity (zero) and initial displacement (zero or results of previous increment).
*Step 2* - Form the internal force vector and the stiffness matrix of each element.
*Step 3* - Assembling the internal force vector.
*Step 4* - Estimate the residual force vector using Eq. (7).
*Step 5* - Go to step 12, if $\left\|\frac{R^T R}{P^T P}\right\| < e_R$. Otherwise, continue.
*Step 6* - Form the artificial mass matrix.
*Step 7* - Form the fictitious damping matrix.
*Step 8* - Update the velocities using Eq. (5).
*Step 9* - Update the time step.
*Step 10* - Update the nodal displacements using Eq. (6).
*Step 11* - Go to step 2.
*Step 12* - Print the displacements for this increment.
*Step 13* - If $N > 10$, the analysis is finished; otherwise continue.
*Step 14* - $N = N + 1$ and go to step 2.

Here, The number of increments is shown with $N$. The acceptable error of residual force ($e_R$) is the same for all schemes, and its value equals $10^{-4}$. It is dimensionless. The thickness of the plates $h$, the elasticity modulus $E$ and Poisson's ratio $\upsilon$ are assumed to be 1 cm, and 200 GPa and 0.3, respectively in all the samples. The dimensionless load parameter is $\frac{12qb^4\left(1-\upsilon^2\right)}{Eh^4}$. In this relation, the uniform load and the width or diameter of the plates are shown with $q$ and $b$, correspondingly. Moreover, the flexural rigidity of plate is obtained from $D = \frac{Eh^3}{12(1-\upsilon^2)}$. The node that has the maximum deflection is shown with the symbol **M** in the figures. Furthermore, the simple boundaries are shown with dashed lines, and the clamped supports are shown in shaded areas. The horizontal axis in the load-displacement curves is the deflection to the thickness ratio. The merit of the various techniques is estimated using the following equation, and it is based on the number of iterations ($E_I$) and the analysis durations ($E_T$).

$$E_I = 100 \times \left(\frac{I_{\max} - I}{I_{\max} - I_{\min}}\right) \tag{46}$$

$$E_T = 100 \times \left(\frac{T_{\max} - T}{T_{\max} - T_{\min}}\right) \tag{47}$$

The number of iterations and the analysis time are shown with I & T, respectively. Zero is the lowest score, and it is associated with a solution that has required the largest number of iterations or the longest time for the analysis. On the other hand, a procedure with the minimum number of iterations or time taken for the analysis is given a score of 100. Then, the results are compared and ranked. Moreover, the authors have suggested other

**Tab. 1.** The used dynamic relaxation methods and their indexes

| Number | Method | Index |
|---|---|---|
| 1 | Papadrakakis | Papadrakakis |
| 2 | Underwood | Underwood |
| 3 | Qiang | Qiang |
| 4 | Zhang 1 | Zhang1 |
| 5 | Zhang 2 | Zhang2 |
| 6 | Nodal Damping | Nodal Damping |
| 7 | Rezaiee-Pajand & Taghavian Hakkak 1 | RPTH1 |
| 8 | Kinetic Damping Dynamic Relaxation | kdDR |
| 9 | Minimizing the residual force | MFT |
| 10 | Rezaiee-Pajand & Alamatian 1 | mdDR1 |
| 11 | Rezaiee-Pajand & Alamatian 2 | mdDR2 |
| 12 | Minimizing the residual Energy | MRE |
| 13 | Rezaiee-Pajand & Sarafrazi | RPS |
| 14 | Zero Damping | zdDR |
| 15 | Dunkerley | Dunkerley |
| 16 | Rezaiee-Pajand & Taghavian Hakkak 2 | RPTH2 |

fictitious parameters for some strategies. Table 1 shows the various methods used in this study. In Zhang1 and Zhang2, the time steps to find the mass matrices are assumed to be 1 and 1.1, correspondingly. Damping is calculated by Zhang approach in RPTH2 tactic. Furthermore, the minimum residual force procedure is used in mdDR2 scheme to obtain the time step.

### 3.1 The quadrilateral plate with various supports

The first, analysis of the quadrilateral plate shown in Fig. 1 is performed in three modes. In two cases, a square plate is considered. One case is clamped while the other structure has simple boundaries. The third plate is a clamped rectangular plate with a length to the width ratio equal to 2. The width of plate $b$ is equal to 1 meter. To study the effect of the mesh, both 10 x 10 and 20 x 20 configurations are used. Due to symmetry, a quarter of plates are modeled. Figs. 2 to 4 show the maximal load-deflection curves. It is worth emphasizing; the maximum displacement is in the middle of the plate. The result obtained from the computer program of the authors is the same as the results reported in Ref. [5].

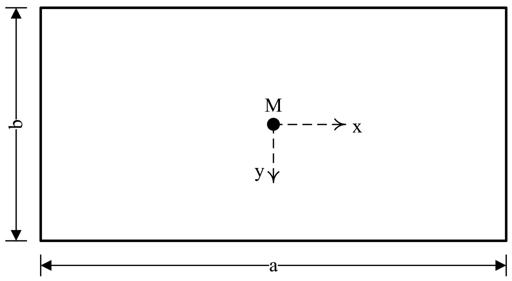


**Fig. 1.** The quadrilateral plate

The number of iterations and the analysis time of the methods are presented in Tables 2 to 7. Based on Table 2, the Rezaiee-Pajand and Taghavian Hakkak approach in the analysis of clamped square plate with 10 x 10 mesh converged to in-

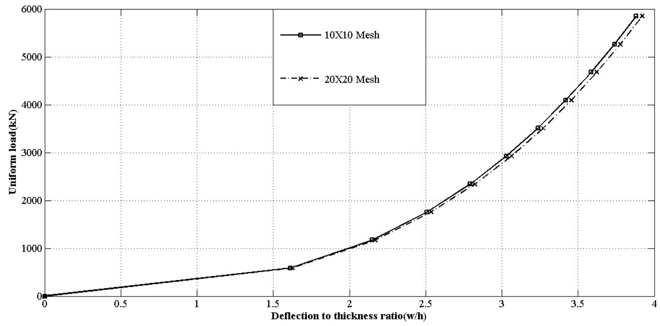


**Fig. 2.** The load- maximum deflection curves for the clamped square plate

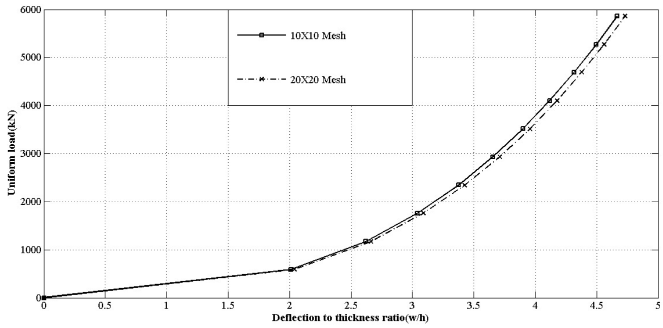


**Fig. 3.** The load- maximum deflection curves for the clamped rectangular plate

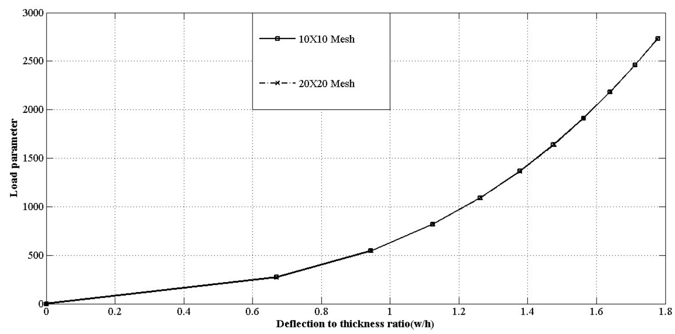


**Fig. 4.** The load- maximum deflection curves for the simple square plate

**Tab. 2.** The ranking of methods for the clamped square plate (mesh 10 X 10)

| Method | Number of iterations in each loading step | | | | | | | | | | Total Iterations | Score | Grade | Time (Second) | Score | Grade |
|---|---|---|---|---|---|---|---|---|---|---|---|---|---|---|---|---|
| | 1 | 2 | 3 | 4 | 5 | 6 | 7 | 8 | 9 | 10 | | | | | | |
| 1 | 1399 | 1275 | 1350 | 1380 | 1441 | 1435 | 1477 | 1199 | 501 | 499 | 11956 | 0 | 13 | 49.11 | 0 | 14 |
| 2 | 272 | 238 | 214 | 201 | 200 | 179 | 217 | 189 | 172 | 165 | 2047 | 100 | 1 | 8.172 | 100 | 1 |
| 3 | 290 | 257 | 240 | 229 | 222 | 216 | 211 | 208 | 205 | 202 | 2280 | 97.649 | 3 | 9.25 | 97.367 | 2 |
| 4 | 300 | 280 | 266 | 258 | 248 | 239 | 234 | 228 | 220 | 219 | 2492 | 95.509 | 6 | 9.843 | 95.918 | 4 |
| 5 | 314 | 294 | 279 | 270 | 261 | 251 | 245 | 239 | 231 | 229 | 2613 | 94.288 | 10 | 10.312 | 94.773 | 8 |
| 6 | 332 | 278 | 251 | 257 | 247 | 239 | 232 | 227 | 222 | 218 | 2503 | 95.398 | 7 | 9.938 | 95.686 | 6 |
| 7 | 172 | 134 | Error | Error | Error | Error | Error | Error | Error | Error | | | 0 | | | 0 |
| 8 | 525 | 443 | 415 | 379 | 371 | 354 | 365 | 373 | 366 | 362 | 3953 | 80.765 | 11 | 19 | 73.55 | 12 |
| 9 | 320 | 295 | 278 | 269 | 259 | 248 | 241 | 238 | 229 | 226 | 2603 | 94.389 | 9 | 10.797 | 93.588 | 11 |
| 10 | 300 | 280 | 265 | 257 | 248 | 239 | 234 | 228 | 220 | 219 | 2490 | 95.529 | 5 | 9.922 | 95.725 | 5 |
| 11 | 343 | 282 | 273 | 256 | 246 | 237 | 229 | 225 | 218 | 217 | 2526 | 95.166 | 8 | 10.625 | 94.008 | 9 |
| 12 | 340 | 282 | 273 | 256 | 246 | 237 | 229 | 225 | 218 | 220 | 2526 | 95.166 | 8 | 10.64 | 93.971 | 10 |
| 13 | 290 | 257 | 240 | 229 | 221 | 215 | 211 | 207 | 204 | 201 | 2275 | 97.699 | 2 | 9.516 | 96.717 | 3 |
| 14 | 305 | 270 | 254 | 243 | 236 | 230 | 226 | 222 | 219 | 217 | 2422 | 96.216 | 4 | 10.125 | 95.229 | 7 |
| 15 | 439 | 464 | 478 | 496 | 503 | 508 | 518 | 522 | 516 | 527 | 4971 | 70.491 | 12 | 19.469 | 72.405 | 13 |
| 16 | 183 | 160 | Error | Error | Error | Error | Error | Error | Error | Error | | | 0 | | | 0 |

**Tab. 3.** The ranking of methods for the clamped square plate (mesh 20 X 20)

| Method | Number of iterations in each loading step | | | | | | | | | | Total Iterations | Score | Grade | Time (Second) | Score | Grade |
|---|---|---|---|---|---|---|---|---|---|---|---|---|---|---|---|---|
| | 1 | 2 | 3 | 4 | 5 | 6 | 7 | 8 | 9 | 10 | | | | | | |
| 1 | 3771 | 3680 | 2867 | 2412 | 2013 | 2561 | 3706 | 2718 | 1879 | 1857 | 27464 | 0 | 13 | 827.141 | 0 | 13 |
| 2 | 701 | 572 | 509 | 475 | 419 | 429 | 413 | 408 | 365 | 362 | 4653 | 100 | 1 | 103.891 | 100 | 1 |
| 3 | 791 | 648 | 589 | 551 | 523 | 502 | 485 | 471 | 460 | 449 | 5469 | 96.423 | 3 | 134.687 | 95.742 | 4 |
| 4 | 828 | 714 | 642 | 624 | 597 | 571 | 552 | 537 | 520 | 508 | 6093 | 93.687 | 6 | 134.844 | 95.72 | 5 |
| 5 | 868 | 750 | 673 | 655 | 627 | 601 | 578 | 563 | 546 | 533 | 6394 | 92.368 | 9 | 141 | 94.869 | 6 |
| 6 | 939 | 705 | 628 | 580 | 546 | 522 | 548 | 532 | 518 | 505 | 6023 | 93.994 | 5 | 133.156 | 95.954 | 2 |
| 7 | 671 | 510 | 452 | Error | Error | Error | Error | Error | Error | Error | | | 0 | | | 0 |
| 8 | 1083 | 938 | 822 | 779 | 706 | 726 | 730 | 626 | 692 | 635 | 7737 | 86.48 | 11 | 187.484 | 88.442 | 10 |
| 9 | 1587 | 749 | 675 | 650 | 625 | 599 | 577 | 562 | 546 | 532 | 7102 | 89.264 | 10 | 184.422 | 88.865 | 9 |
| 10 | 827 | 714 | 643 | 623 | 597 | 574 | 551 | 537 | 521 | 508 | 6095 | 93.678 | 7 | 134.485 | 95.77 | 3 |
| 11 | 863 | 714 | 643 | 623 | 597 | 572 | 551 | 537 | 521 | 508 | 6129 | 93.529 | 8 | 160.437 | 92.182 | 7 |
| 12 | Fail | Fail | Fail | Fail | Fail | Fail | Fail | Fail | Fail | Fail | | | 0 | | | 0 |
| 13 | 791 | 648 | 589 | 551 | 523 | 502 | 485 | 471 | 459 | 449 | 5468 | 96.427 | 2 | 182.562 | 89.123 | 8 |
| 14 | 805 | 661 | 634 | 591 | 562 | 538 | 520 | 485 | 473 | 463 | 5732 | 95.27 | 4 | 191.546 | 87.88 | 11 |
| 15 | 951 | 983 | 1003 | 1039 | 1044 | 1053 | 1067 | 1084 | 1063 | 1082 | 10369 | 74.942 | 12 | 227.563 | 82.901 | 12 |
| 16 | 692 | 559 | 490 | Fail | Fail | Fail | Fail | Fail | Fail | Fail | | | 0 | | | 0 |

correct answers after the third increment. In other words, this tactic achieves acceptable error, but the answers are incorrect. On the other hand, Table 3 shows that the minimum residual energy procedure (MRE) is not able to obtain an acceptable error. Hence, it is divergent. RPTH2 solution is similar to that after the third increment. Moreover, RPTH1 process after third increment gives incorrect answers.

As shown in Tables 4 and 5, Rezaiee-Pajand and Taghavian Hakkak technique is not useful for the rectangular plate. Furthermore, in the 20 x 20 configuration for this structure, the MFT strategy yields an inappropriate response from the beginning. The results obtained for the clamped supports show that the mdDR2 and MRE methods require the same number of iterations. In these algorithms, a similar relationship is used for estimating the mass and damping. It is worth noting that if Eq. (38) has no real answer, the calculated time step by the MRF approach is used in the MRE tactic. Thus, it can conclude that for these plates, the minimum unbalanced energy scheme is unsuitable for calculating the time step. In other words, the minimum residual force is used to find this parameter. This has happened after the fifth increment for a rectangular plate with a 10 x 10 mesh.

The MdDR1 and Zhang1 algorithms more or less have the same performance. This behavior can be for the reason that in both techniques, the fictitious frequency is estimated by using Rayleigh principle. The MFT and Zhang2 techniques approximately require the same number of iterations. However, the number of iterations is different in each loading increment. It is worth emphasizing; these two procedures also use Rayleigh principle to estimate the smallest frequency. Table 3 shows that the number of iterations of the first increment of these two strategies is significantly different. Their numbers of iterations are different at each incremental loading since the time step for these two methods is different. It should be noted that the mass and damping matrices have a greater effect on the dynamic relaxation process. Hence, the total numbers of iterations of other increments of these two tactics get close to each other.

Moreover, Qiang and RPS approaches have the same behavior. As mentioned in the RPS technique, the minimum calculated eigenvalue by Rayleigh principle, and the iterative power procedure is utilized to find the damping. Qiang scheme also uses Rayleigh principle. Hence, it is concluded that in analysis of these structures, the minimum frequency by using Rayleigh principle is always less when compared with the iterative power algorithm.

The results of analysis of simple square plates are inserted in Tables 6 and 7. These tables show that all the methods converge to an acceptable answer. What was mentioned above about the similar behavior of some of the tactics more or less holds true here. The results obtained indicate that Underwood approach is the most efficient one and Papadrakakis process is the worst procedure to solve the quadrilateral plate problem. The mesh used does not have a significant effect on the response as shown in Fig. 2 to 4. Hence, a similar configuration is used for the other samples.

## 3.2 The circular plate

In this section, the circular plate, showed in Fig. 5, is analyzed. Due to the symmetry, one-quarter of the structure is modeled. The number of used bending elements is 67. The results of the analysis are shown in Fig. 6 and inserted in Table 8. According to the Table 8, Rezaiee-Pajand and Taghavian Hakkak technique is not able to solve this plate. In other words, the residual force in these methods is more than the acceptable value. For this reason, this approach diverges. Hence, the ranking of this strategy is zero. It should be noted that the similar behavior observed for some of the schemes in the previous problem is also seen in this sample. Based on the obtained results, Underwood and Qiang procedures are the best and Papadrakakis algorithm is the worst tactic to solve this problem.

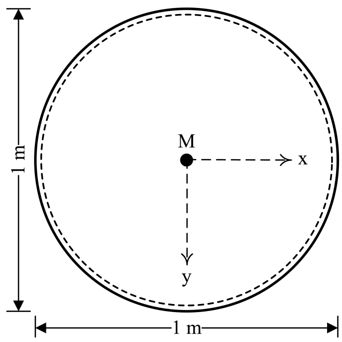


**Fig. 5.** The circular plate

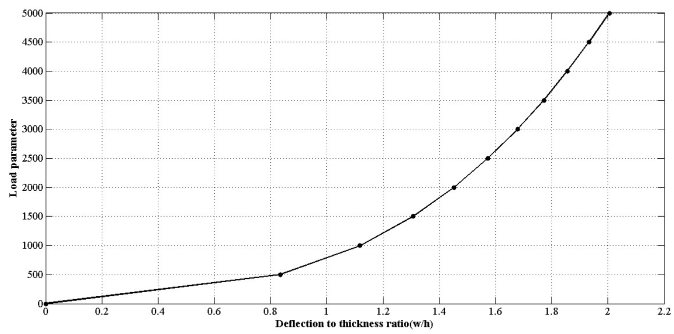


**Fig. 6.** The load- maximum deflection curve for the circular plate

## 3.3 The rectangular plate with opening

Now, the quadrilateral plate with opening shown in Fig. 7 is investigated. Rezaiee-Pajand and Alamatian have analyzed this structure before [41]. In the current paper, this plate will be solved with 20 X 20 mesh. Maximum displacement occurs in the middle of the upper boundary. The load-maximum deflection curve is shown in Fig. 8. The achieved responses are the same as those reported by Ref [41]. The ranking of the methods is inserted in Table 9. Based on Table 9, the responses of RPTH2 and RPTH1 processes are divergent. The MRE and mdDR2 approaches are the most efficient tactics to analyze this plate. The

**Tab. 4.** The ranking of methods for the clamped rectangular plate (mesh 10 X 10)

| Method | Number of iterations in each loading step | | | | | | | | | | Total Iterations | Score | Grade | Time (Second) | Score | Grade |
|---|---|---|---|---|---|---|---|---|---|---|---|---|---|---|---|---|
| | 1 | 2 | 3 | 4 | 5 | 6 | 7 | 8 | 9 | 10 | | | | | | |
| 1 | 1340 | 1151 | 1350 | 2215 | 755 | 790 | 822 | 927 | 911 | 1023 | 11284 | 0 | 14 | 46.297 | 0 | 14 |
| 2 | 284 | 243 | 200 | 203 | 214 | 218 | 221 | 247 | 221 | 201 | 2252 | 100 | 1 | 8.859 | 100 | 1 |
| 3 | 309 | 286 | 281 | 284 | 292 | 301 | 311 | 320 | 328 | 336 | 3048 | 91.187 | 10 | 12.296 | 90.819 | 9 |
| 4 | 316 | 286 | 265 | 251 | 242 | 234 | 227 | 221 | 217 | 214 | 2473 | 97.553 | 3 | 9.704 | 97.743 | 3 |
| 5 | 331 | 300 | 278 | 261 | 254 | 246 | 239 | 232 | 228 | 223 | 2592 | 96.236 | 7 | 10.188 | 96.45 | 6 |
| 6 | 344 | 293 | 274 | 263 | 256 | 246 | 242 | 237 | 230 | 225 | 2610 | 96.036 | 8 | 10.062 | 96.787 | 5 |
| 7 | Fail | Fail | Fail | Fail | Fail | Fail | Fail | Fail | Fail | Fail | | | 0 | | | 0 |
| 8 | 525 | 459 | 411 | 409 | 412 | 385 | 411 | 409 | 425 | 433 | 4279 | 77.558 | 12 | 20.344 | 69.323 | 12 |
| 9 | 276 | 299 | 274 | 265 | 260 | 251 | 245 | 240 | 232 | 229 | 2571 | 96.468 | 6 | 10.359 | 95.993 | 7 |
| 10 | 315 | 286 | 269 | 252 | 242 | 234 | 228 | 224 | 217 | 213 | 2480 | 97.476 | 4 | 9.562 | 98.122 | 2 |
| 11 | 268 | 284 | 259 | 252 | 246 | 238 | 233 | 225 | 221 | 216 | 2442 | 97.896 | 2 | 9.797 | 97.495 | 4 |
| 12 | 333 | 292 | 275 | 268 | 246 | 238 | 233 | 225 | 228 | 216 | 2554 | 96.656 | 5 | 10.469 | 95.7 | 8 |
| 13 | 309 | 285 | 280 | 283 | 291 | 300 | 310 | 319 | 327 | 335 | 3039 | 91.287 | 9 | 12.344 | 90.691 | 10 |
| 14 | 326 | 302 | 298 | 302 | 311 | 322 | 333 | 344 | 353 | 362 | 3253 | 88.917 | 11 | 13.359 | 87.98 | 11 |
| 15 | 577 | 589 | 599 | 600 | 595 | 603 | 598 | 605 | 602 | 606 | 5974 | 58.791 | 13 | 22.828 | 62.688 | 13 |
| 16 | Fail | Fail | Fail | Fail | Fail | Fail | Fail | Fail | Fail | Fail | | | 0 | | | 0 |

**Tab. 5.** The ranking of methods for the clamped rectangular plate (mesh 20 X 20)

| Method | Number of iterations in each loading step | | | | | | | | | | Total Iterations | Score | Grade | Time (Second) | Score | Grade |
|---|---|---|---|---|---|---|---|---|---|---|---|---|---|---|---|---|
| | 1 | 2 | 3 | 4 | 5 | 6 | 7 | 8 | 9 | 10 | | | | | | |
| 1 | 3246 | 3312 | 3266 | 3060 | 3470 | 4576 | 4793 | 5186 | 3503 | 4048 | 38460 | 0 | 11 | 1157.454 | 0 | 13 |
| 2 | 689 | 548 | 488 | 482 | 432 | 460 | 439 | 433 | 408 | 357 | 4736 | 100 | 1 | 105.969 | 100 | 1 |
| 3 | 788 | 663 | 611 | 578 | 555 | 536 | 522 | 510 | 499 | 491 | 5753 | 96.984 | 3 | 141.969 | 96.576 | 6 |
| 4 | 826 | 716 | 649 | 606 | 579 | 555 | 537 | 521 | 508 | 497 | 5994 | 96.27 | 5 | 134.078 | 97.327 | 2 |
| 5 | 866 | 750 | 680 | 636 | 607 | 582 | 563 | 546 | 532 | 522 | 6284 | 95.41 | 7 | 140.844 | 96.683 | 4 |
| 6 | 936 | 715 | 646 | 605 | 609 | 587 | 570 | 555 | 541 | 530 | 6294 | 95.38 | 8 | 141.031 | 96.665 | 5 |
| 7 | Fail | Fail | Fail | Fail | Fail | Fail | Fail | Fail | Fail | Fail | | | 0 | | | 0 |
| 8 | 1126 | 907 | 810 | 799 | 750 | 738 | 756 | 692 | 685 | 670 | 7933 | 90.52 | 9 | 193.141 | 91.71 | 9 |
| 9 | Error | Error | Error | Error | Error | Error | Error | Error | Error | Error | | | 0 | | | 0 |
| 10 | 826 | 716 | 649 | 606 | 579 | 555 | 537 | 521 | 508 | 497 | 5994 | 96.27 | 5 | 134.594 | 97.278 | 3 |
| 11 | 828 | 716 | 649 | 606 | 579 | 555 | 537 | 521 | 508 | 497 | 5996 | 96.264 | 6 | 158.625 | 94.992 | 7 |
| 12 | 828 | 716 | 649 | 606 | 579 | 555 | 537 | 521 | 508 | 497 | 5996 | 96.264 | 6 | 159.328 | 94.925 | 8 |
| 13 | 788 | 662 | 611 | 578 | 554 | 536 | 521 | 509 | 499 | 490 | 5748 | 96.999 | 2 | 195.297 | 91.505 | 10 |
| 14 | 815 | 677 | 627 | 594 | 570 | 552 | 538 | 526 | 516 | 507 | 5922 | 96.483 | 4 | 200.922 | 90.97 | 11 |
| 15 | 1159 | 1175 | 1232 | 1254 | 1263 | 1271 | 1281 | 1293 | 1308 | 1291 | 12527 | 76.898 | 10 | 279.625 | 83.485 | 12 |
| 16 | Fail | Fail | Fail | Fail | Fail | Fail | Fail | Fail | Fail | Fail | | | 0 | | | 0 |

**Tab. 6.** The ranking of methods for the simple square plate (mesh 10 X 10)

| Method | Number of iterations in each loading step | | | | | | | | | | Total Iterations | Score | Grade | Time (Second) | Score | Grade |
|---|---|---|---|---|---|---|---|---|---|---|---|---|---|---|---|---|
| | 1 | 2 | 3 | 4 | 5 | 6 | 7 | 8 | 9 | 10 | | | | | | |
| 1 | 1652 | 801 | 777 | 815 | 855 | 566 | 518 | 572 | 723 | 706 | 7985 | 0 | 16 | 33.891 | 0 | 16 |
| 2 | 205 | 176 | 137 | 128 | 171 | 137 | 108 | 115 | 85 | 91 | 1353 | 100 | 1 | 5.484 | 100 | 1 |
| 3 | 259 | 197 | 174 | 161 | 151 | 144 | 139 | 135 | 132 | 129 | 1621 | 95.959 | 8 | 6.75 | 95.543 | 9 |
| 4 | 228 | 192 | 164 | 148 | 158 | 151 | 143 | 137 | 132 | 130 | 1583 | 96.532 | 4 | 6.329 | 97.025 | 4 |
| 5 | 239 | 201 | 173 | 177 | 144 | 157 | 150 | 144 | 139 | 136 | 1660 | 95.371 | 11 | 6.641 | 95.927 | 7 |
| 6 | 305 | 191 | 163 | 147 | 134 | 150 | 143 | 137 | 132 | 130 | 1632 | 95.793 | 10 | 6.375 | 96.863 | 6 |
| 7 | 250 | 191 | 167 | 152 | 142 | 134 | 128 | 124 | 119 | 116 | 1523 | 97.437 | 2 | 6.281 | 97.194 | 3 |
| 8 | 324 | 183 | 250 | 243 | 201 | 212 | 204 | 191 | 202 | 184 | 2194 | 87.319 | 15 | 10.625 | 81.902 | 15 |
| 9 | 277 | 198 | 175 | 164 | 155 | 148 | 141 | 141 | 136 | 132 | 1667 | 95.265 | 12 | 7.031 | 94.554 | 12 |
| 10 | 228 | 192 | 165 | 148 | 159 | 151 | 144 | 138 | 132 | 130 | 1587 | 96.472 | 5 | 6.343 | 96.976 | 5 |
| 11 | 277 | 198 | 166 | 156 | 148 | 135 | 135 | 134 | 130 | 124 | 1603 | 96.23 | 6 | 6.75 | 95.543 | 9 |
| 12 | 285 | 198 | 178 | 156 | 151 | 135 | 135 | 134 | 130 | 125 | 1627 | 95.869 | 9 | 6.907 | 94.991 | 11 |
| 13 | 259 | 197 | 174 | 160 | 151 | 144 | 139 | 135 | 131 | 129 | 1619 | 95.989 | 7 | 6.906 | 94.994 | 10 |
| 14 | 268 | 206 | 183 | 169 | 160 | 154 | 148 | 144 | 141 | 139 | 1712 | 94.587 | 13 | 7.313 | 93.561 | 13 |
| 15 | 222 | 192 | 191 | 196 | 180 | 195 | 186 | 200 | 192 | 190 | 1944 | 91.089 | 14 | 7.765 | 91.97 | 14 |
| 16 | 221 | 189 | 159 | 166 | 156 | 147 | 140 | 135 | 129 | 125 | 1567 | 96.773 | 3 | 6.219 | 97.413 | 2 |

**Tab. 7.** The ranking of methods for the simple square plate (mesh 20 X 20)

| Method | Number of iterations in each loading step | | | | | | | | | | Total Iterations | Score | Grade | Time (Second) | Score | Grade |
|---|---|---|---|---|---|---|---|---|---|---|---|---|---|---|---|---|
| | 1 | 2 | 3 | 4 | 5 | 6 | 7 | 8 | 9 | 10 | | | | | | |
| 1 | 6947 | 5590 | 4744 | 5384 | 4274 | 3975 | 3422 | 2780 | 3866 | 3605 | 44587 | 0 | 16 | 1425.875 | 0 | 16 |
| 2 | 766 | 573 | 549 | 464 | 461 | 373 | 376 | 391 | 350 | 358 | 4661 | 100 | 1 | 107 | 100 | 1 |
| 3 | 923 | 694 | 605 | 551 | 513 | 485 | 463 | 446 | 431 | 418 | 5529 | 97.826 | 7 | 138.047 | 97.646 | 7 |
| 4 | 840 | 698 | 598 | 533 | 492 | 457 | 502 | 480 | 461 | 443 | 5504 | 97.889 | 3 | 125.078 | 98.629 | 3 |
| 5 | 881 | 732 | 621 | 560 | 510 | 479 | 526 | 504 | 483 | 465 | 5761 | 97.245 | 12 | 130.469 | 98.221 | 5 |
| 6 | 1178 | 701 | 587 | 522 | 482 | 528 | 502 | 481 | 462 | 373 | 5816 | 97.107 | 13 | 132.407 | 98.074 | 6 |
| 7 | 949 | 713 | 620 | 563 | 524 | 494 | 471 | 452 | 436 | 422 | 5644 | 97.538 | 10 | 141.422 | 97.39 | 9 |
| 8 | 775 | 610 | 580 | 666 | 562 | 586 | 472 | 530 | 522 | 525 | 5828 | 97.077 | 14 | 142.344 | 97.32 | 10 |
| 9 | 916 | 720 | 620 | 559 | 553 | 496 | 461 | 470 | 458 | 451 | 5704 | 97.388 | 11 | 153.406 | 96.481 | 13 |
| 10 | 840 | 698 | 593 | 533 | 486 | 456 | 435 | 480 | 398 | 382 | 5301 | 98.397 | 2 | 120.609 | 98.968 | 2 |
| 11 | 898 | 687 | 596 | 540 | 524 | 495 | 471 | 445 | 433 | 419 | 5508 | 97.879 | 4 | 148.625 | 96.844 | 11 |
| 12 | 898 | 687 | 596 | 540 | 524 | 496 | 471 | 445 | 433 | 419 | 5509 | 97.876 | 5 | 149.016 | 96.814 | 12 |
| 13 | 923 | 694 | 605 | 551 | 513 | 485 | 463 | 445 | 430 | 418 | 5527 | 97.831 | 6 | 195.422 | 93.296 | 14 |
| 14 | 931 | 702 | 613 | 559 | 522 | 494 | 472 | 454 | 439 | 427 | 5613 | 97.616 | 8 | 200.063 | 92.944 | 15 |
| 15 | 1372 | 598 | 531 | 539 | 494 | 532 | 505 | 485 | 530 | 516 | 6102 | 96.391 | 15 | 140.172 | 97.485 | 8 |
| 16 | 861 | 718 | 615 | 553 | 497 | 538 | 514 | 416 | 474 | 456 | 5642 | 97.543 | 9 | 128.125 | 98.398 | 4 |

**Tab. 8.** The ranking of methods for the circular plate

| Method | Number of iterations in each loading step | | | | | | | | | | Total Iterations | Score | Grade | Time (Second) | Score | Grade |
|---|---|---|---|---|---|---|---|---|---|---|---|---|---|---|---|---|
| | 1 | 2 | 3 | 4 | 5 | 6 | 7 | 8 | 9 | 10 | | | | | | |
| 1 | 1543 | 983 | 981 | 978 | 1008 | 1054 | 1224 | 1409 | 1588 | 1823 | 12591 | 0 | 16 | 632.484 | 0 | 16 |
| 2 | 392 | 355 | 342 | 267 | 291 | 266 | 258 | 274 | 253 | 269 | 2967 | 89.501 | 3 | 103.906 | 93.003 | 3 |
| 3 | 444 | 390 | 363 | 344 | 331 | 320 | 312 | 305 | 299 | 294 | 3402 | 85.455 | 12 | 145.094 | 85.756 | 11 |
| 4 | 327 | 334 | 327 | 315 | 308 | 298 | 295 | 287 | 281 | 277 | 3049 | 88.738 | 4 | 106.593 | 92.53 | 4 |
| 5 | 343 | 351 | 344 | 330 | 320 | 313 | 309 | 301 | 294 | 290 | 3195 | 87.38 | 10 | 111.828 | 91.609 | 7 |
| 6 | 355 | 344 | 314 | 326 | 311 | 298 | 286 | 278 | 296 | 291 | 3099 | 88.273 | 8 | 108.609 | 92.176 | 6 |
| 7 | 318 | 247 | 215 | 196 | 183 | 173 | 166 | 160 | 155 | 206 | 2019 | 98.317 | 2 | 85.719 | 96.203 | 2 |
| 8 | 715 | 637 | 582 | 554 | 505 | 475 | 493 | 466 | 457 | 456 | 5340 | 67.432 | 14 | 208.375 | 74.622 | 12 |
| 9 | 314 | 356 | 343 | 329 | 319 | 313 | 307 | 301 | 294 | 288 | 3164 | 87.669 | 9 | 144.281 | 85.899 | 10 |
| 10 | 326 | 334 | 328 | 315 | 308 | 299 | 295 | 287 | 281 | 277 | 3050 | 88.729 | 5 | 106.688 | 92.514 | 5 |
| 11 | 347 | 334 | 328 | 315 | 305 | 299 | 295 | 287 | 281 | 277 | 3068 | 88.561 | 6 | 139.937 | 86.664 | 8 |
| 12 | 366 | 334 | 328 | 315 | 305 | 299 | 295 | 287 | 281 | 277 | 3087 | 88.385 | 7 | 141.562 | 86.378 | 9 |
| 13 | 443 | 389 | 362 | 344 | 331 | 320 | 312 | 305 | 299 | 294 | 3399 | 85.483 | 11 | 217.844 | 72.956 | 13 |
| 14 | 460 | 403 | 376 | 358 | 345 | 335 | 326 | 319 | 314 | 309 | 3545 | 84.125 | 13 | 227.297 | 71.293 | 14 |
| 15 | 830 | 901 | 939 | 964 | 990 | 1015 | 1027 | 1042 | 1046 | 1072 | 9826 | 25.714 | 15 | 343.641 | 50.822 | 15 |
| 16 | 235 | 216 | 201 | 188 | 182 | 174 | 168 | 161 | 158 | 155 | 1838 | 100 | 1 | 64.14 | 100 | 1 |

**Tab. 9.** The ranking of methods for the rectangular plate with opening

| Method | Number of iterations in each loading step | | | | | | | | | | Total Iterations | Score | Grade | Time (Second) | Score | Grade |
|---|---|---|---|---|---|---|---|---|---|---|---|---|---|---|---|---|
| | 1 | 2 | 3 | 4 | 5 | 6 | 7 | 8 | 9 | 10 | | | | | | |
| 1 | 2440 | 1869 | 2549 | 2060 | 2255 | 2458 | 2165 | 1553 | 1419 | 1134 | 19902 | 0 | 13 | 1227.25 | 0 | 14 |
| 2 | 578 | 511 | 509 | 489 | 410 | 439 | 426 | 356 | 377 | 381 | 4476 | 99.478 | 4 | 183.469 | 99.553 | 3 |
| 3 | 906 | 826 | 773 | 742 | 721 | 705 | 694 | 685 | 678 | 673 | 7403 | 80.602 | 10 | 398.922 | 79.004 | 10 |
| 4 | 579 | 503 | 465 | 444 | 425 | 417 | 401 | 394 | 388 | 379 | 4395 | 100 | 1 | 180.313 | 99.854 | 2 |
| 5 | 607 | 528 | 488 | 465 | 446 | 438 | 420 | 413 | 407 | 398 | 4610 | 98.614 | 5 | 188.343 | 99.088 | 4 |
| 6 | 664 | 527 | 484 | 494 | 476 | 461 | 454 | 440 | 421 | 415 | 4836 | 97.156 | 7 | 198.359 | 98.133 | 5 |
| 7 | Fail | Fail | Fail | Fail | Fail | Fail | Fail | Fail | Fail | Fail | | | 0 | | | 0 |
| 8 | 968 | 800 | 741 | 718 | 670 | 678 | 640 | 606 | 623 | 621 | 7065 | 82.782 | 8 | 314.281 | 87.076 | 9 |
| 9 | 623 | 528 | 488 | 464 | 446 | 429 | 420 | 413 | 405 | 396 | 4612 | 98.601 | 6 | 268.922 | 91.403 | 8 |
| 10 | 579 | 504 | 465 | 445 | 425 | 418 | 401 | 394 | 388 | 380 | 4399 | 99.974 | 2 | 178.781 | 100 | 1 |
| 11 | 597 | 504 | 465 | 445 | 425 | 418 | 401 | 394 | 388 | 380 | 4417 | 99.858 | 3 | 259.016 | 92.347 | 6 |
| 12 | 597 | 504 | 465 | 445 | 425 | 418 | 401 | 394 | 388 | 380 | 4417 | 99.858 | 3 | 260.016 | 92.252 | 7 |
| 13 | 906 | 825 | 773 | 741 | 720 | 705 | 693 | 685 | 678 | 672 | 7398 | 80.635 | 9 | 658.938 | 54.204 | 12 |
| 14 | 931 | 851 | 800 | 769 | 748 | 733 | 723 | 714 | 708 | 703 | 7680 | 78.816 | 11 | 690.594 | 51.185 | 13 |
| 15 | 1126 | 1172 | 1217 | 1247 | 1274 | 1281 | 1310 | 1317 | 1323 | 1332 | 12599 | 47.095 | 12 | 519.437 | 67.509 | 11 |
| 16 | Fail | Fail | Fail | Fail | Fail | Fail | Fail | Fail | Fail | Fail | | | 0 | | | 0 |

numbers of iterations required in these two methods are the same in all increments. The reason for this behavior was reported earlier. Moreover, Papadrakakis algorithm consumes the longest time. The similarity in the behavior of the techniques reported earlier also holds true here.

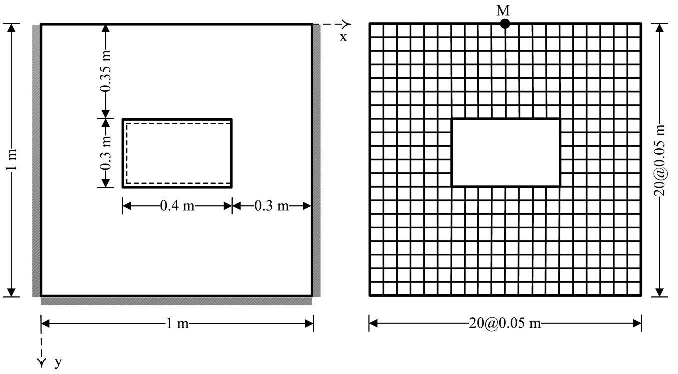


**Fig. 7.** The rectangular plate with opening

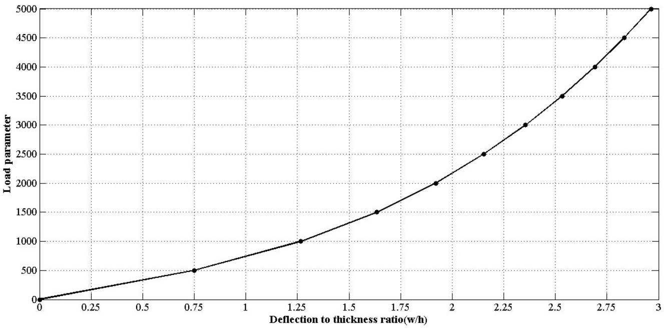


**Fig. 8.** The load- maximum deflection curves for the rectangular plate with opening

### 3.4 The L-shaped plate

Here, an L-shaped plate, which is shown in Fig. 9, is analyzed [39]. This structure is modeled with 150 bending elements. Some symbols are used for boundary conditions. Free boundaries, clamped and simple supports are displayed by F, C and S, respectively. For example, a plate SFSSSF has a free edge on the borders 2 and 6, and the other edges are simple support. The load-maximum deflection curves are shown in Fig. 10. The maximum displacement of CSCSSS and CCCCCC plates occurs at a node with coordinates $(0.5, 0.5)$ m. On the other hand; this node is in the middle of the edge 2 of the SFSSSF structure. Tables 10 to 12 include the rating and ranking of the methods. The number of iterations and the required time to converge in Rezaiee-Pajand and Taghavian Hakkak approach are less than the other techniques for the CSCSSS and CCCCCC plates. Moreover, Zhang1 and mdDR1 procedures are the best solutions for the analysis of the SFSSSF structure. It should be noted that these two schemes have the same behavior. Table 11 shows that Rezaiee-Pajand and Taghavian Hakkak tactic is not able to analyze the SFSSSF plate. Papadrakakis process requires the largest number of iterations and the longest time to converge among the strategies that converged.

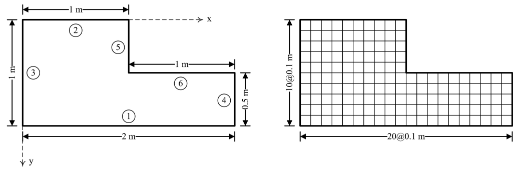


**Fig. 9.** The L- shaped plate

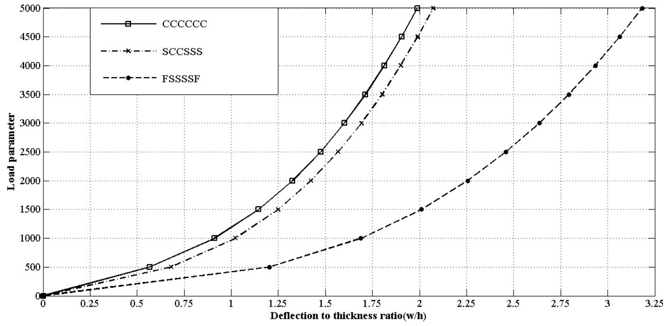


**Fig. 10.** The load- maximum deflection curves for the L- shaped plate

### 3.5 The triangular plate

Now, the triangular plate shown in Fig. 11 will be investigated. Sixty bending elements are used for the structural analysis. Fig. 12 shows the load-displacement curve. The maximum deflection occurs in the middle of the triangle. The results are inserted in Table 13. Underwood method requires the lowest number of iterations, and the shortest time required to analyze this plate. On the other hand, the rank of RPTH1 and RPTH2 is zero. In other words, these techniques are diverged from the first step. The similar behaviors of some tactics that in first sample have been discussed are also true here.

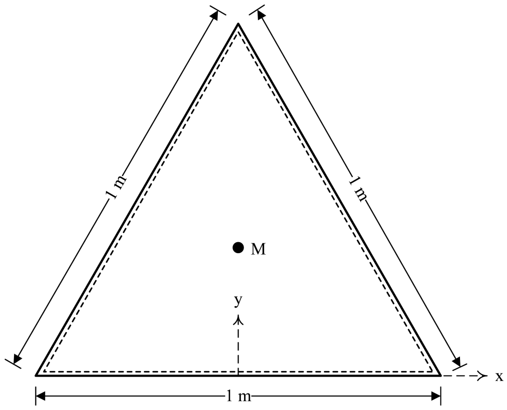


**Fig. 11.** The triangular plate

### 3.6 Parallelogram plate

Fig. 13 shows a parallelogram plate, and the mesh used in this article. The results are shown in Table 14 and Fig. 14. Based on Table 14, RPTH1 and RPTH2 approaches were not able to achieve acceptable residual errors. In other words, the responses were divergent. Hence, the ranking of these techniques is zero. On the other hand, Underwood, mdDR1 and Zhang1 methods have the first to the third rankings for the number of iterations, respectively. It is worth emphasizing; Zhang1 and mdDR1 so-

**Tab. 10.** The ranking of methods for CCCCCC plate

| Method | Number of iterations in each loading step | | | | | | | | | | Total Iterations | Score | Grade | Time (Second) | Score | Grade |
|---|---|---|---|---|---|---|---|---|---|---|---|---|---|---|---|---|
| | 1 | 2 | 3 | 4 | 5 | 6 | 7 | 8 | 9 | 10 | | | | | | |
| 1 | 1966 | 1092 | 1481 | 7682 | 5149 | 816 | 829 | 832 | 864 | 872 | 21583 | 0 | 16 | 1097.203 | 0 | 16 |
| 2 | 424 | 373 | 300 | 300 | 323 | 303 | 286 | 267 | 269 | 284 | 3129 | 93.937 | 3 | 119.938 | 95.063 | 5 |
| 3 | 478 | 409 | 380 | 362 | 348 | 338 | 330 | 323 | 317 | 312 | 3597 | 91.555 | 11 | 169.188 | 90.272 | 10 |
| 4 | 357 | 360 | 341 | 328 | 317 | 304 | 296 | 288 | 284 | 280 | 3155 | 93.805 | 4 | 119.687 | 95.088 | 4 |
| 5 | 607 | 528 | 488 | 465 | 446 | 438 | 420 | 413 | 407 | 398 | 4610 | 86.399 | 13 | 188.343 | 88.409 | 11 |
| 6 | 425 | 375 | 346 | 324 | 332 | 322 | 313 | 304 | 298 | 292 | 3331 | 92.909 | 9 | 120.375 | 95.021 | 6 |
| 7 | 340 | 258 | 227 | 208 | 195 | 186 | 178 | 172 | 167 | 279 | 2210 | 98.615 | 2 | 99.563 | 97.045 | 2 |
| 8 | 695 | 594 | 614 | 534 | 486 | 449 | 490 | 491 | 463 | 462 | 5278 | 82.998 | 14 | 212.375 | 86.071 | 12 |
| 9 | 365 | 371 | 357 | 343 | 332 | 318 | 309 | 301 | 297 | 294 | 3287 | 93.133 | 8 | 159.156 | 91.248 | 9 |
| 10 | 356 | 361 | 342 | 328 | 317 | 305 | 296 | 288 | 284 | 280 | 3157 | 93.795 | 5 | 114.266 | 95.615 | 3 |
| 11 | 388 | 361 | 341 | 328 | 317 | 305 | 296 | 288 | 284 | 280 | 3188 | 93.637 | 6 | 154.453 | 91.706 | 7 |
| 12 | 412 | 361 | 341 | 328 | 317 | 305 | 296 | 288 | 284 | 280 | 3212 | 93.515 | 7 | 155.969 | 91.558 | 8 |
| 13 | 478 | 409 | 380 | 361 | 348 | 338 | 329 | 322 | 317 | 311 | 3593 | 91.575 | 10 | 249.468 | 82.463 | 13 |
| 14 | 495 | 424 | 395 | 377 | 364 | 354 | 345 | 339 | 333 | 328 | 3754 | 90.756 | 12 | 261.219 | 81.32 | 14 |
| 15 | 886 | 962 | 1003 | 1018 | 1051 | 1054 | 1079 | 1090 | 1099 | 1111 | 10353 | 57.165 | 15 | 373.656 | 70.383 | 15 |
| 16 | 259 | 233 | 212 | 198 | 187 | 178 | 174 | 170 | 165 | 162 | 1938 | 100 | 1 | 69.187 | 100 | 1 |

**Tab. 11.** The ranking of methods for SFSSSF plate

| Method | Number of iterations in each loading step | | | | | | | | | | Total Iterations | Score | Grade | Time (Second) | Score | Grade |
|---|---|---|---|---|---|---|---|---|---|---|---|---|---|---|---|---|
| | 1 | 2 | 3 | 4 | 5 | 6 | 7 | 8 | 9 | 10 | | | | | | |
| 1 | 7666 | 13501 | 6969 | 12199 | 5390 | 5709 | 8489 | 5538 | 9861 | 11601 | 86923 | 0 | 12 | 23363.859 | 0 | 14 |
| 2 | 1396 | 1284 | 1074 | 1237 | 940 | 1112 | 827 | 911 | 1022 | 940 | 10743 | 99.487 | 4 | 789.735 | 99.89 | 3 |
| 3 | 2034 | 2037 | 1998 | 1941 | 1887 | 1839 | 1797 | 1761 | 1729 | 1701 | 18724 | 89.064 | 10 | 2802.485 | 90.984 | 11 |
| 4 | 1399 | 1136 | 1080 | 1051 | 1016 | 989 | 966 | 950 | 931 | 912 | 10430 | 99.896 | 3 | 775.594 | 99.953 | 2 |
| 5 | 1467 | 1188 | 1134 | 1103 | 1066 | 1032 | 1012 | 997 | 974 | 958 | 10931 | 99.241 | 7 | 800.672 | 99.842 | 4 |
| 6 | 1322 | 1171 | 1165 | 1097 | 1031 | 1079 | 1052 | 1025 | 1000 | 975 | 10917 | 99.26 | 6 | 802.344 | 99.834 | 5 |
| 7 | Fail | Fail | Fail | Fail | Fail | Fail | Fail | Fail | Fail | Fail | | | 0 | | | 0 |
| 8 | 1949 | 1844 | 1519 | 1645 | 1538 | 1578 | 1565 | 1591 | 1369 | 1333 | 15931 | 92.712 | 8 | 1229.64 | 97.944 | 6 |
| 9 | 1402 | 1193 | 1144 | 1108 | 1070 | 1038 | 1015 | 997 | 977 | 958 | 10902 | 99.279 | 5 | 1750.906 | 95.637 | 10 |
| 10 | 1399 | 1132 | 1080 | 1051 | 1015 | 984 | 963 | 950 | 929 | 913 | 10416 | 99.914 | 2 | 764.937 | 100 | 1 |
| 11 | 1307 | 1137 | 1089 | 1051 | 1015 | 989 | 967 | 950 | 932 | 913 | 10350 | 100 | 1 | 1700.421 | 95.86 | 9 |
| 12 | 1307 | 1137 | 1089 | 1051 | 1015 | 989 | 967 | 950 | 932 | 913 | 10350 | 100 | 1 | 1694.469 | 95.887 | 8 |
| 13 | 2034 | 2037 | 1998 | 1941 | 1887 | 1839 | 1797 | 1761 | 1729 | 1701 | 18724 | 89.064 | 10 | 7920.516 | 68.337 | 13 |
| 14 | 2057 | 2060 | 2023 | 1968 | 1915 | 1867 | 1826 | 1790 | 1759 | 1731 | 18996 | 88.709 | 11 | 7559.203 | 69.935 | 12 |
| 15 | 1571 | 1649 | 1683 | 1702 | 1727 | 1746 | 1761 | 1774 | 1790 | 1791 | 17194 | 91.062 | 9 | 1272.313 | 97.755 | 7 |
| 16 | Fail | Fail | Fail | Fail | Fail | Fail | Fail | Fail | Fail | Fail | | | 0 | | | 0 |

**Tab. 12.** The ranking of methods for CSCSSS plate

| Method | Number of iterations in each loading step | | | | | | | | | | Total Iterations | Score | Grade | Time (Second) | Score | Grade |
|---|---|---|---|---|---|---|---|---|---|---|---|---|---|---|---|---|
| | 1 | 2 | 3 | 4 | 5 | 6 | 7 | 8 | 9 | 10 | | | | | | |
| 1 | 13588 | 9215 | 12627 | 10460 | 11797 | 11320 | 12603 | 10115 | 8373 | 10220 | 110318 | 15.998 | 10 | 5005.109 | 19.328 | 10 |
| 2 | 2232 | 2013 | 1828 | 1696 | 1746 | 1628 | 1615 | 1777 | 1656 | 1410 | 17601 | 100 | 1 | 709.094 | 100 | 1 |
| 3 | 12730 | 12596 | 12629 | 12576 | 12489 | 12387 | 12281 | 12175 | 12071 | 11969 | 123903 | 3.6901 | 12 | 5425.625 | 11.432 | 11 |
| 4 | 7156 | 6850 | 6778 | 6696 | 6612 | 6531 | 6453 | 6380 | 6311 | 6245 | 66012 | 56.14 | 8 | 2664.187 | 63.287 | 7 |
| 5 | 7503 | 7183 | 7108 | 7022 | 6934 | 6849 | 6768 | 6691 | 6618 | 6549 | 69225 | 53.229 | 9 | 2816.516 | 60.426 | 9 |
| 6 | 7909 | 6814 | 6065 | 5676 | 5377 | 5073 | 4808 | 4633 | 4547 | 4415 | 55317 | 65.829 | 5 | 2253.157 | 71.005 | 5 |
| 7 | Fail | Fail | Fail | Fail | Fail | Fail | Fail | Fail | Fail | Fail | | | 0 | | | 0 |
| 8 | 3039 | 2235 | 1959 | 2209 | 1907 | 1842 | 1864 | 1852 | 2267 | 1752 | 20926 | 96.988 | 2 | 888.235 | 96.636 | 2 |
| 9 | 2803 | 3320 | 5970 | 2444 | 1813 | 2172 | 1879 | 2106 | 1514 | 1667 | 25688 | 92.673 | 3 | 1136.438 | 91.975 | 3 |
| 10 | 7155 | 6849 | 6777 | 6695 | 6611 | 6530 | 6452 | 6379 | 6309 | 6244 | 66001 | 56.149 | 7 | 2695.547 | 62.698 | 8 |
| 11 | 6579 | 6297 | 5995 | 5991 | 5802 | 5521 | 5336 | 4079 | 6276 | 6235 | 58111 | 63.298 | 6 | 2567.765 | 65.097 | 6 |
| 12 | 2416 | Fail | Fail | Fail | Fail | Fail | Fail | Fail | Fail | Fail | | | 0 | | | 0 |
| 13 | 12727 | 12591 | 12623 | 12570 | 12482 | 12380 | 12273 | 12167 | 12062 | 11960 | 123835 | 3.7518 | 11 | 5813.203 | 4.1538 | 12 |
| 14 | 13020 | 12931 | 13001 | 12974 | 12905 | 12819 | 12725 | 12629 | 12533 | 12439 | 127976 | 0 | 13 | 6034.406 | 0 | 13 |
| 15 | 4995 | 3884 | 3355 | 2998 | 2731 | 2521 | 2348 | 2201 | 2075 | 1964 | 29072 | 89.607 | 4 | 1193.359 | 90.906 | 4 |
| 16 | Fail | Fail | Fail | Fail | Fail | Fail | Fail | Fail | Fail | Fail | | | 0 | | | 0 |

**Tab. 13.** The ranking of methods for the triangular plate

| Method | Number of iterations in each loading step | | | | | | | | | | Total Iterations | Score | Grade | Time (Second) | Score | Grade |
|---|---|---|---|---|---|---|---|---|---|---|---|---|---|---|---|---|
| | 1 | 2 | 3 | 4 | 5 | 6 | 7 | 8 | 9 | 10 | | | | | | |
| 1 | 8963 | 7892 | 6264 | 5930 | 7527 | 9460 | 7559 | 5706 | 4146 | 4674 | 68121 | 0 | 12 | 1988.375 | 0 | 14 |
| 2 | 1056 | 898 | 666 | 701 | 620 | 688 | 700 | 685 | 671 | 564 | 7249 | 100 | 1 | 202.984 | 100 | 1 |
| 3 | 1888 | 1551 | 1427 | 1351 | 1299 | 1260 | 1229 | 1204 | 1183 | 1164 | 13556 | 89.639 | 10 | 391.61 | 89.435 | 11 |
| 4 | 1270 | 1131 | 1025 | 950 | 905 | 864 | 832 | 805 | 785 | 766 | 9333 | 96.576 | 3 | 261.078 | 96.746 | 2 |
| 5 | 1332 | 1180 | 1073 | 995 | 951 | 906 | 864 | 840 | 823 | 805 | 9769 | 95.86 | 5 | 274.828 | 95.976 | 5 |
| 6 | 1767 | 1326 | 1174 | 1113 | 1053 | 1028 | 1025 | 979 | 980 | 953 | 11398 | 93.184 | 7 | 324.172 | 93.212 | 9 |
| 7 | Fail | Fail | Fail | Fail | Fail | Fail | Fail | Fail | Fail | Fail | | | 0 | | | 0 |
| 8 | 1632 | 1224 | 1373 | 1234 | 1131 | 993 | 1073 | 1085 | 928 | 993 | 11666 | 92.744 | 8 | 351.547 | 91.679 | 10 |
| 9 | 1502 | 1180 | 1073 | 993 | 947 | 906 | 864 | 840 | 823 | 805 | 9933 | 95.591 | 6 | 294.719 | 94.862 | 8 |
| 10 | 1270 | 1132 | 1026 | 946 | 906 | 863 | 823 | 806 | 785 | 771 | 9328 | 96.585 | 2 | 262.296 | 96.678 | 3 |
| 11 | 1390 | 1131 | 1025 | 945 | 905 | 863 | 823 | 806 | 785 | 771 | 9444 | 96.394 | 4 | 278.875 | 95.749 | 6 |
| 12 | 1390 | 1131 | 1025 | 945 | 905 | 863 | 823 | 806 | 785 | 771 | 9444 | 96.394 | 4 | 280.859 | 95.638 | 7 |
| 13 | 1887 | 1551 | 1427 | 1351 | 1299 | 1259 | 1229 | 1203 | 1182 | 1164 | 13552 | 89.645 | 9 | 410.906 | 88.354 | 12 |
| 14 | 1914 | 1575 | 1452 | 1377 | 1325 | 1286 | 1256 | 1231 | 1210 | 1193 | 13819 | 89.207 | 11 | 423.985 | 87.622 | 13 |
| 15 | 1456 | 874 | 856 | 871 | 896 | 881 | 901 | 901 | 900 | 908 | 9444 | 96.394 | 4 | 265.359 | 96.506 | 4 |
| 16 | Fail | Fail | Fail | Fail | Fail | Fail | Fail | Fail | Fail | Fail | | | 0 | | | 0 |

**Tab. 14.** The ranking of methods for the parallelogram plate

| Method | Number of iterations in each loading step | | | | | | | | | | Total Iterations | Score | Grade | Time (Second) | Score | Grade |
|---|---|---|---|---|---|---|---|---|---|---|---|---|---|---|---|---|
| | 1 | 2 | 3 | 4 | 5 | 6 | 7 | 8 | 9 | 10 | | | | | | |
| 1 | 15964 | 6676 | 6564 | 6118 | 5447 | 5832 | 5377 | 6245 | 6435 | 6487 | 71145 | 0 | 12 | 2741.328 | 0 | 14 |
| 2 | 1167 | 846 | 787 | 725 | 685 | 618 | 585 | 565 | 558 | 543 | 7079 | 100 | 1 | 261.469 | 100 | 1 |
| 3 | 1298 | 1030 | 924 | 858 | 811 | 776 | 747 | 724 | 704 | 687 | 8559 | 97.69 | 2 | 323.437 | 97.501 | 2 |
| 4 | 1169 | 1132 | 1006 | 926 | 874 | 825 | 796 | 773 | 744 | 717 | 8962 | 97.061 | 5 | 323.609 | 97.494 | 3 |
| 5 | 1226 | 1186 | 1053 | 973 | 915 | 866 | 835 | 801 | 781 | 758 | 9394 | 96.387 | 8 | 338.093 | 96.91 | 6 |
| 6 | 1750 | 1144 | 993 | 911 | 911 | 868 | 835 | 809 | 783 | 762 | 9766 | 95.806 | 9 | 353.266 | 96.298 | 9 |
| 7 | Fail | Fail | Fail | Fail | Fail | Fail | Fail | Fail | Fail | Fail | | | 0 | | | 0 |
| 8 | 1578 | 1362 | 1279 | 1039 | 1018 | 1037 | 950 | 959 | 891 | 910 | 11023 | 93.844 | 10 | 427.75 | 93.295 | 12 |
| 9 | 3643 | 1186 | 1053 | 973 | 915 | 866 | 835 | 801 | 770 | 758 | 11800 | 92.631 | 11 | 455.563 | 92.173 | 13 |
| 10 | 1168 | 1133 | 1006 | 927 | 874 | 827 | 790 | 765 | 744 | 717 | 8951 | 97.078 | 4 | 323.734 | 97.489 | 4 |
| 11 | 1613 | 1132 | 1006 | 926 | 874 | 827 | 790 | 765 | 744 | 717 | 9394 | 96.387 | 8 | 363.297 | 95.894 | 11 |
| 12 | 1456 | 1132 | 1006 | 926 | 874 | 827 | 790 | 765 | 744 | 717 | 9237 | 96.632 | 6 | 358.281 | 96.096 | 10 |
| 13 | 1298 | 1030 | 924 | 858 | 811 | 776 | 747 | 724 | 704 | 687 | 8559 | 97.69 | 2 | 341.859 | 96.758 | 7 |
| 14 | 1313 | 1043 | 937 | 871 | 824 | 789 | 761 | 738 | 718 | 701 | 8695 | 97.478 | 3 | 347.359 | 96.536 | 8 |
| 15 | 1720 | 839 | 832 | 839 | 839 | 823 | 847 | 831 | 854 | 845 | 9269 | 96.582 | 7 | 335.485 | 97.015 | 5 |
| 16 | Fail | Fail | Fail | Fail | Fail | Fail | Fail | Fail | Fail | Fail | | | 0 | | | 0 |

**Tab. 15.** The ranking of methods for the heterogeneous quadrilateral plate I

| Method | Number of iterations in each loading step | | | | | | | | | | Total Iterations | Score | Grade | Time (Second) | Score | Grade |
|---|---|---|---|---|---|---|---|---|---|---|---|---|---|---|---|---|
| | 1 | 2 | 3 | 4 | 5 | 6 | 7 | 8 | 9 | 10 | | | | | | |
| 1 | 10755 | 26064 | 11281 | 9888 | 10493 | 13845 | 8447 | 8176 | 7186 | 14534 | 120669 | 0 | 13 | 7610.969 | 0 | 14 |
| 2 | 2077 | 1473 | 1337 | 1237 | 1276 | 1236 | 1203 | 1175 | 1176 | 1170 | 13360 | 100 | 1 | 703.891 | 100 | 1 |
| 3 | 7748 | 6838 | 6380 | 6081 | 5865 | 5698 | 5564 | 5453 | 5358 | 5277 | 60262 | 56.293 | 11 | 3463.719 | 60.043 | 11 |
| 4 | 2368 | 2113 | 1942 | 1824 | 1747 | 1697 | 1644 | 1602 | 1565 | 1524 | 18026 | 95.652 | 2 | 937.984 | 96.611 | 2 |
| 5 | 2483 | 2217 | 2037 | 1925 | 1834 | 1779 | 1725 | 1681 | 1652 | 1599 | 18932 | 94.808 | 7 | 985.36 | 95.925 | 6 |
| 6 | 2926 | 2161 | 1959 | 1834 | 1773 | 1696 | 1645 | 1594 | 1574 | 1540 | 18702 | 95.022 | 6 | 973.234 | 96.1 | 4 |
| 7 | Fail | Fail | Fail | Fail | Fail | Fail | Fail | Fail | Fail | Fail | | | 0 | | | 0 |
| 8 | 3311 | 2260 | 2154 | 1864 | 2091 | 1887 | 1872 | 1811 | 1827 | 1516 | 20593 | 93.26 | 9 | 1122.781 | 93.935 | 9 |
| 9 | 2502 | 2216 | 2037 | 1925 | 1848 | 1780 | 1725 | 1682 | 1648 | 1599 | 18962 | 94.78 | 8 | 1142.688 | 93.647 | 10 |
| 10 | 2368 | 2113 | 1941 | 1825 | 1747 | 1697 | 1644 | 1602 | 1565 | 1525 | 18027 | 95.651 | 3 | 948.39 | 96.46 | 3 |
| 11 | 2411 | 2113 | 1941 | 1836 | 1747 | 1697 | 1644 | 1603 | 1575 | 1525 | 18092 | 95.59 | 4 | 1066.516 | 94.75 | 7 |
| 12 | 2411 | 2113 | 1941 | 1836 | 1747 | 1697 | 1644 | 1603 | 1575 | 1525 | 18092 | 95.59 | 4 | 1069.844 | 94.702 | 8 |
| 13 | 7748 | 6837 | 6379 | 6080 | 5864 | 5697 | 5562 | 5451 | 5357 | 5276 | 60251 | 56.303 | 10 | 4241.485 | 48.783 | 12 |
| 14 | 7848 | 6946 | 6494 | 6198 | 5985 | 5820 | 5687 | 5578 | 5485 | 5405 | 61446 | 55.189 | 12 | 4364.5 | 47.002 | 13 |
| 15 | 4861 | 2895 | 2146 | 1674 | 1232 | 1124 | 1183 | 1120 | 1179 | 1173 | 18587 | 95.129 | 5 | 975.297 | 96.071 | 5 |
| 16 | Fail | Fail | Fail | Fail | Fail | Fail | Fail | Fail | Fail | Fail | | | 0 | | | 0 |

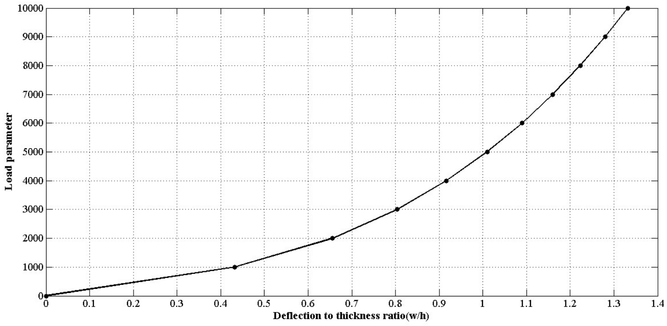


**Fig. 12.** The load- maximum deflection curves for the triangular plate

lutions have the same behavior.

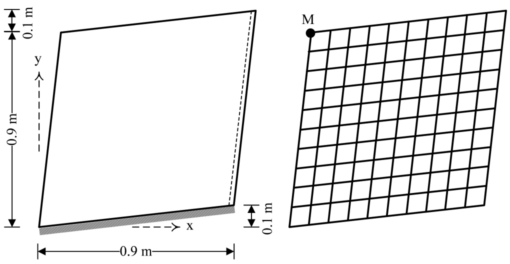


**Fig. 13.** The parallelogram plate

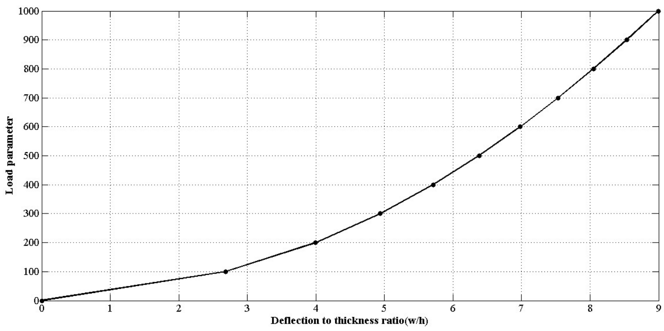


**Fig. 14.** The load- maximum deflection curves for the parallelogram plate

### 3.7 The heterogeneous quadrilateral plate I

The quadrilateral plate shown in Fig. 15 will be solved here. The number of elements is 233. Fig. 16 indicates load-deflection curve at node M. The coordinates of this node are (0.42, 0.24) m. Table 15 lists the ranking of all strategies. Based on this table, RPTH1 and RPTH2 methods are not capable of analyzing this structure. Underwood, Zhang1 and mdDR1 processes are the best ones for the analysis of this plate. Papadrakakis method is the worst one. It should be noted that some schemes have a similar behavior.

### 3.8 The heterogeneous quadrilateral plate II

A quadrilateral plate shown in Fig. 17 will be analyzed. Fig. 18 shows its load-maximum deflection curve. The plate was modeled with 108 elements. The maximum displacement occurs in the middle of the free edge. Moreover, the ranking of each tactic is inserted in Table 16. According to this table, the residual forces in both RPTH procedures are infinity. Hence,

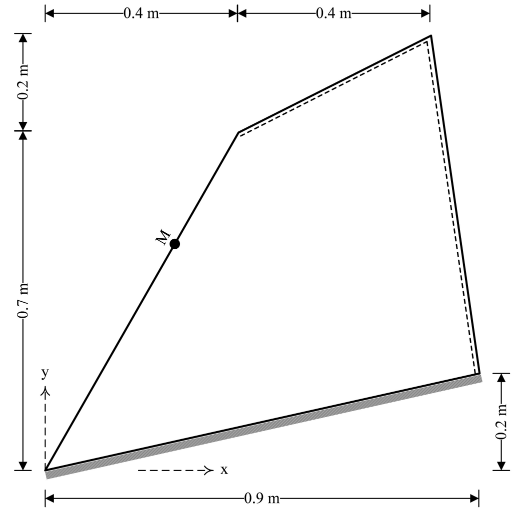


**Fig. 15.** The heterogeneous quadrilateral plate I

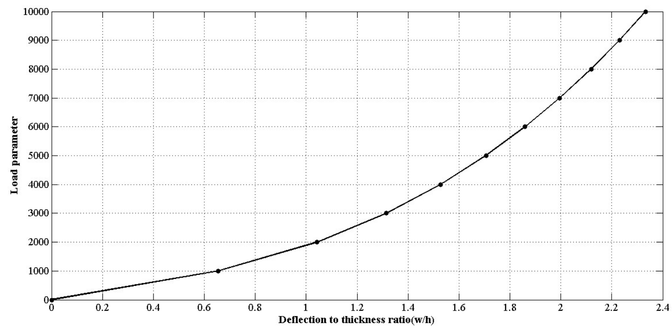


**Fig. 16.** The load- deflection curves for the heterogeneous quadrilateral plate I

these algorithms are not able to converge to the answer. Top ranking approaches for this sample are the same as the parallelogram plate.

### 3.9 The elliptical plate

Fig. 19 shows the elliptical plate. Due to symmetry, 64 bending plate elements are used to discretize a quarter of the structure. The maximum deflection occurs at the center. Results of the analysis are presented in Fig. 20 and Table 17. Underwood method is the best and Papadrakakis algorithm is the worst process among the converged techniques. Both RPTH schemes could not solve this structure.

### 3.10 The donut-shaped plate

Here, the plate in Fig. 21 is studied. Due to the symmetry, meshing is done in a quarter of the structure with 90 elements. Fig. 22 shows the load-maximum deflection curve. Table 18 demonstrates the rating of methods. Underwood procedure is the most efficient solution to analyze this structure. In other words, this approach requires the lowest number of iterations and the shortest time to yield a response. RPTH2 and RPTH1 strategies are not able to solve this plate. Also, Papadrakakis tactic takes the maximum number of iterations and the longest duration analysis.

**Tab. 16.** The ranking of methods for the heterogeneous quadrilateral plate II

| Method | Number of iterations in each loading step | | | | | | | | | | Total Iterations | Score | Grade | Time (Second) | Score | Grade |
|---|---|---|---|---|---|---|---|---|---|---|---|---|---|---|---|---|
| | 1 | 2 | 3 | 4 | 5 | 6 | 7 | 8 | 9 | 10 | | | | | | |
| 1 | 3034 | 1767 | 2604 | 3224 | 1853 | 1595 | 2074 | 2267 | 1173 | 1337 | 20928 | 0 | 13 | 472.312 | 0 | 14 |
| 2 | 479 | 408 | 382 | 372 | 294 | 315 | 322 | 332 | 283 | 286 | 3473 | 100 | 1 | 76.688 | 100 | 1 |
| 3 | 559 | 486 | 451 | 428 | 412 | 400 | 390 | 382 | 375 | 369 | 4252 | 95.537 | 3 | 95.515 | 95.241 | 2 |
| 4 | 622 | 539 | 493 | 465 | 444 | 426 | 409 | 400 | 391 | 379 | 4568 | 93.727 | 6 | 100.203 | 94.056 | 4 |
| 5 | 652 | 564 | 518 | 486 | 466 | 445 | 430 | 419 | 409 | 398 | 4787 | 92.472 | 9 | 105.078 | 92.824 | 9 |
| 6 | 712 | 561 | 525 | 502 | 482 | 470 | 459 | 460 | 448 | 449 | 5068 | 90.862 | 10 | 111.265 | 91.26 | 11 |
| 7 | Fail | Fail | Fail | Fail | Fail | Fail | Fail | Fail | Fail | Fail | | | 0 | | | 0 |
| 8 | 813 | 651 | 625 | 572 | 573 | 570 | 564 | 541 | 560 | 488 | 5957 | 85.769 | 11 | 151.188 | 81.169 | 13 |
| 9 | 672 | 541 | 512 | 480 | 458 | 440 | 428 | 415 | 408 | 397 | 4751 | 92.678 | 8 | 108.875 | 91.864 | 10 |
| 10 | 622 | 539 | 493 | 465 | 444 | 426 | 410 | 400 | 389 | 379 | 4567 | 93.732 | 5 | 100.688 | 93.934 | 5 |
| 11 | 631 | 539 | 493 | 464 | 444 | 426 | 410 | 400 | 389 | 379 | 4575 | 93.687 | 7 | 104.469 | 92.978 | 7 |
| 12 | 631 | 539 | 493 | 464 | 444 | 426 | 410 | 400 | 389 | 379 | 4575 | 93.687 | 7 | 104.766 | 92.903 | 8 |
| 13 | 559 | 486 | 451 | 428 | 412 | 400 | 390 | 381 | 374 | 368 | 4249 | 95.554 | 2 | 98.469 | 94.495 | 3 |
| 14 | 573 | 500 | 465 | 443 | 427 | 415 | 405 | 397 | 390 | 384 | 4399 | 94.695 | 4 | 102.563 | 93.46 | 6 |
| 15 | 627 | 650 | 668 | 681 | 691 | 697 | 694 | 708 | 700 | 719 | 6835 | 80.739 | 12 | 150.188 | 81.422 | 12 |
| 16 | Fail | Fail | Fail | Fail | Fail | Fail | Fail | Fail | Fail | Fail | | | 0 | | | 0 |

**Tab. 17.** The ranking of methods for the elliptical plate

| Method | Number of iterations in each loading step | | | | | | | | | | Total Iterations | Score | Grade | Time (Second) | Score | Grade |
|---|---|---|---|---|---|---|---|---|---|---|---|---|---|---|---|---|
| | 1 | 2 | 3 | 4 | 5 | 6 | 7 | 8 | 9 | 10 | | | | | | |
| 1 | 49311 | 38371 | 26186 | 21391 | 19104 | 21316 | 19984 | 23577 | 21011 | 18562 | 258813 | 0 | 13 | 30012.974 | 0 | 14 |
| 2 | 1360 | 1506 | 1481 | 1323 | 1136 | 1292 | 1150 | 1231 | 1227 | 1114 | 12820 | 99.443 | 6 | 1738.703 | 99.468 | 4 |
| 3 | 2152 | 2129 | 2137 | 2131 | 2120 | 2109 | 2101 | 2098 | 2100 | 2105 | 21182 | 96.063 | 10 | 3466.157 | 93.391 | 10 |
| 4 | 1914 | 1484 | 1111 | 1111 | 1056 | 1039 | 1019 | 1002 | 985 | 966 | 11687 | 99.901 | 3 | 1587.594 | 100 | 1 |
| 5 | 2007 | 1557 | 1163 | 1163 | 1109 | 1089 | 1070 | 1048 | 1030 | 1015 | 12251 | 99.673 | 5 | 1664.296 | 99.73 | 3 |
| 6 | 3514 | 3234 | 3016 | 3072 | 2671 | 2889 | 2673 | 2937 | 2535 | 2449 | 28990 | 92.906 | 12 | 3941.5 | 91.719 | 11 |
| 7 | Fail | Fail | Fail | Fail | Fail | Fail | Fail | Fail | Fail | Fail | | | 0 | | | 0 |
| 8 | 2071 | 2038 | 2203 | 1945 | 1887 | 1754 | 1673 | 1648 | 1604 | 1688 | 18511 | 97.142 | 8 | 2609.766 | 96.404 | 9 |
| 9 | 1839 | 1477 | 1163 | 1163 | 1109 | 1089 | 1070 | 1048 | 1030 | 1015 | 12003 | 99.773 | 4 | 2096.891 | 98.208 | 8 |
| 10 | 1913 | 1484 | 1109 | 1108 | 1057 | 1038 | 1019 | 1002 | 985 | 966 | 11681 | 99.903 | 2 | 1591.25 | 99.987 | 2 |
| 11 | 1829 | 1332 | 1109 | 1108 | 1056 | 1038 | 1019 | 1000 | 985 | 966 | 11442 | 100 | 1 | 2002.344 | 98.541 | 6 |
| 12 | 1829 | 1332 | 1109 | 1108 | 1056 | 1038 | 1019 | 1000 | 985 | 966 | 11442 | 100 | 1 | 2002.985 | 98.539 | 7 |
| 13 | 2152 | 2129 | 2137 | 2131 | 2119 | 2109 | 2101 | 2098 | 2100 | 2105 | 21181 | 96.063 | 9 | 5271.782 | 87.039 | 12 |
| 14 | 2174 | 2148 | 2159 | 2154 | 2144 | 2135 | 2129 | 2127 | 2129 | 2136 | 21435 | 95.96 | 11 | 5336.594 | 86.811 | 13 |
| 15 | 1350 | 1392 | 1423 | 1434 | 1447 | 1462 | 1474 | 1492 | 1500 | 1507 | 14481 | 98.771 | 7 | 1970.563 | 98.653 | 5 |
| 16 | Fail | Fail | Fail | Fail | Fail | Fail | Fail | Fail | Fail | Fail | | | 0 | | | 0 |

**Tab. 18.** The ranking of methods for the donut-shaped plate

| Method | Number of iterations in each loading step | | | | | | | | | | Total Iterations | Score | Grade | Time (Second) | Score | Grade |
|---|---|---|---|---|---|---|---|---|---|---|---|---|---|---|---|---|
| | 1 | 2 | 3 | 4 | 5 | 6 | 7 | 8 | 9 | 10 | | | | | | |
| 1 | 9436 | 18643 | 12520 | 9765 | 10678 | 11020 | 11948 | 15918 | 9532 | 16255 | 125715 | 0 | 14 | 8381.609 | 0 | 14 |
| 2 | 1897 | 1931 | 1759 | 2181 | 1989 | 2319 | 2324 | 2315 | 1807 | 2353 | 20875 | 100 | 1 | 1181.453 | 100 | 1 |
| 3 | 5822 | 6820 | 7584 | 8330 | 9097 | 9895 | 10726 | 11590 | 12482 | 13398 | 95744 | 28.587 | 12 | 5696.875 | 37.287 | 11 |
| 4 | 2105 | 2220 | 2193 | 2154 | 2124 | 2139 | 2144 | 2113 | 2102 | 2168 | 21462 | 99.44 | 3 | 1213.422 | 99.556 | 2 |
| 5 | 2208 | 2324 | 2299 | 2263 | 2225 | 2235 | 2249 | 2212 | 2208 | 2271 | 22494 | 98.456 | 6 | 1268.437 | 98.792 | 4 |
| 6 | 2445 | 2411 | 2405 | 2416 | 2428 | 2239 | 2299 | 2354 | 2394 | 2394 | 23785 | 97.224 | 8 | 1349.375 | 97.668 | 6 |
| 7 | Fail | Fail | Fail | Fail | Fail | Fail | Fail | Fail | Fail | Fail | | | 0 | | | 0 |
| 8 | 2817 | 3361 | 3040 | 3482 | 3013 | 2904 | 2977 | 2501 | 2688 | 2700 | 29483 | 91.789 | 9 | 1709.859 | 92.661 | 9 |
| 9 | 2363 | 2324 | 2299 | 2263 | 2225 | 2235 | 2249 | 2212 | 2208 | 2271 | 22649 | 98.308 | 7 | 1404.421 | 96.903 | 8 |
| 10 | 2105 | 2215 | 2189 | 2155 | 2124 | 2128 | 2145 | 2112 | 2103 | 2168 | 21444 | 99.457 | 2 | 1214.391 | 99.543 | 3 |
| 11 | 2520 | 2215 | 2189 | 2155 | 2124 | 2128 | 2143 | 2112 | 2103 | 2168 | 21857 | 99.063 | 5 | 1348.953 | 97.674 | 5 |
| 12 | 2512 | 2215 | 2189 | 2155 | 2124 | 2128 | 2143 | 2112 | 2103 | 2168 | 21849 | 99.071 | 4 | 1350.641 | 97.65 | 7 |
| 13 | 5822 | 6820 | 7583 | 8329 | 9096 | 9894 | 10725 | 11589 | 12481 | 13396 | 95735 | 28.596 | 11 | 6920.922 | 20.287 | 12 |
| 14 | 5875 | 6892 | 7673 | 8435 | 9219 | 10034 | 10883 | 11766 | 12678 | 13614 | 97069 | 27.324 | 13 | 7026.344 | 18.823 | 13 |
| 15 | 5996 | 4969 | 4579 | 4430 | 4401 | 4441 | 4526 | 4642 | 4777 | 4926 | 47687 | 74.426 | 10 | 2697.516 | 78.944 | 10 |
| 16 | Fail | Fail | Fail | Fail | Fail | Fail | Fail | Fail | Fail | Fail | | | 0 | | | 0 |

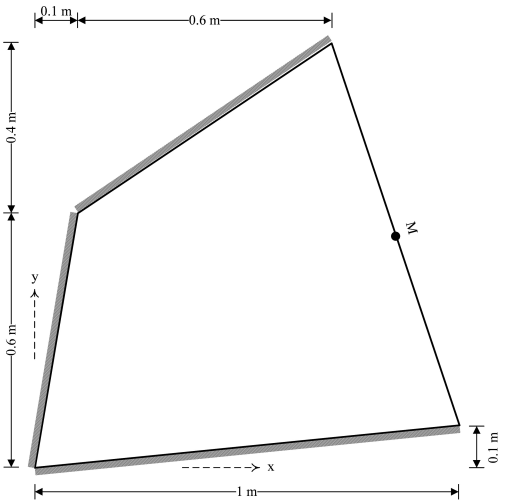


**Fig. 17.** The heterogeneous quadrilateral plate II

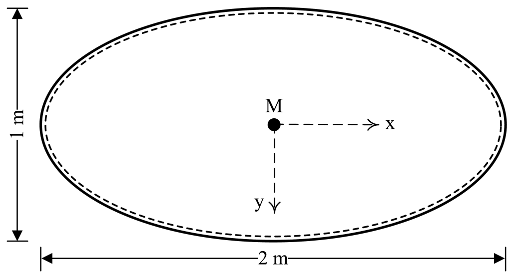


**Fig. 19.** The elliptical plate

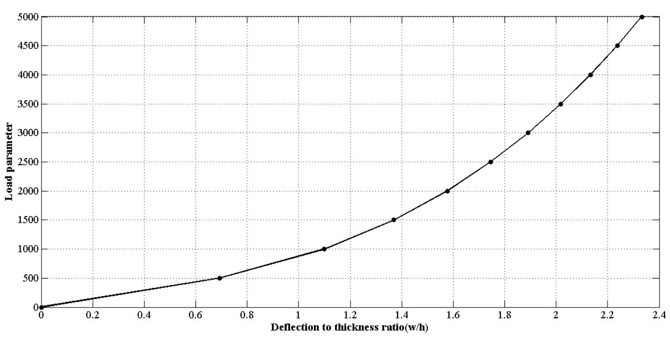


**Fig. 18.** The load- maximum deflection curves for the heterogeneous quadrilateral plate II

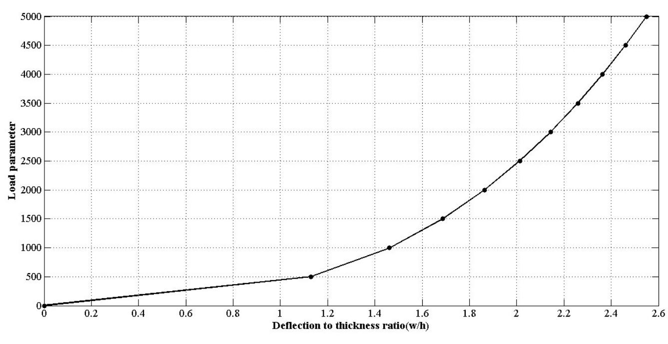


**Fig. 20.** The load- maximum deflection curves for the elliptical plate

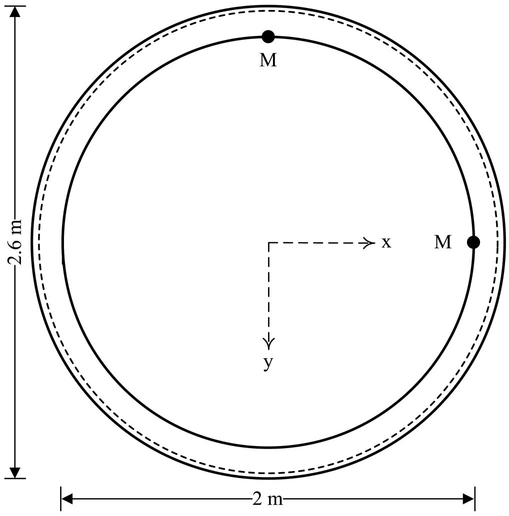


**Fig. 21.** The donut-shaped plate

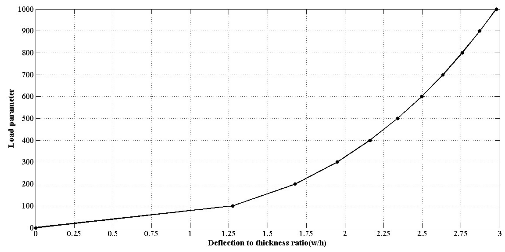


**Fig. 22.** The load- maximum deflection curves for the donut-shaped plate

### 3.11 The plate with arched edges

A quadrilateral plate with two arched edges is analyzed. Fig. 23 shows this structure. The right edge is a circle with a radius of 0.5 m, and the left boundary is a three-point arc. The number of used bending elements for this plate is 74. Fig. 23 shows the location of maximal deflection. The coordinates of this node are (-0.25, 0) m. Fig. 24 and Table 19 present the results. As it was the case for the previous samples, both RPTH methods are not able to converge to a proper answer. Moreover, the MRE technique diverges after the first increment. Underwood procedure and the kinetic dynamic relaxation process are the most efficient solutions for the analysis of this plate, while Papadrakakis algorithm is the worst method. It is worth emphasizing; Zhang1 and mdDR1 schemes as well as Qiang and RPS strategies have a similar behavior.

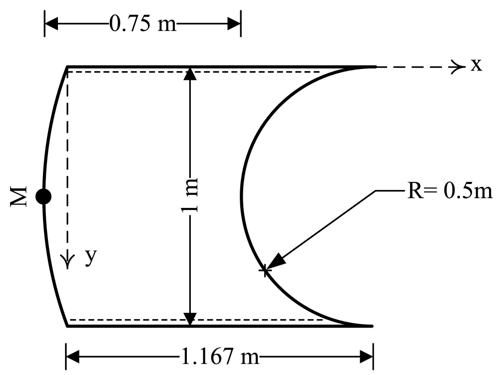


**Fig. 23.** The plate with arched edges

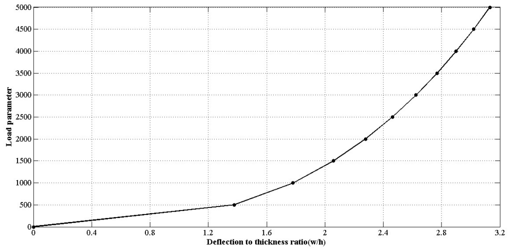


**Fig. 24.** The load- maximum deflection curves for the plate with arched-shape edges

### 3.12 The circular plate with rectangular opening

Dynamic relaxation processes are used for the analysis of circular plates shown in Fig. 25. This structure has a quadrilateral opening. The meshing is done in one-quarter of the plate due to the geometrical and loading symmetry. The number of elements used is 52. Fig. 26 portrays the load- maximum displacement curve. The number of iterations and the analysis time are inserted in Table 20. Underwood and mdDR1 methods are the most appropriate ones to solve this problem.

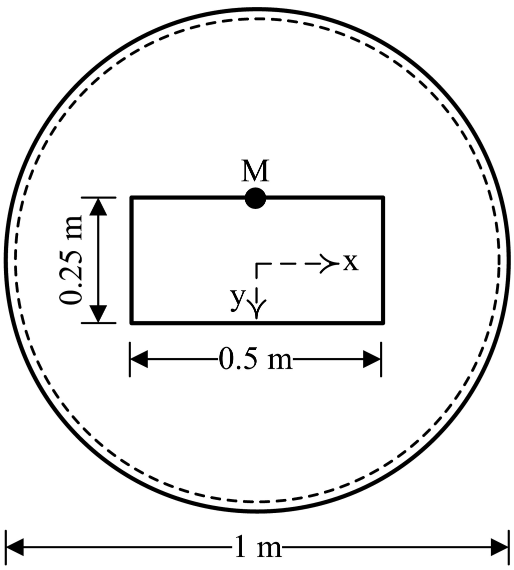


**Fig. 25.** The circular plate with rectangular opening

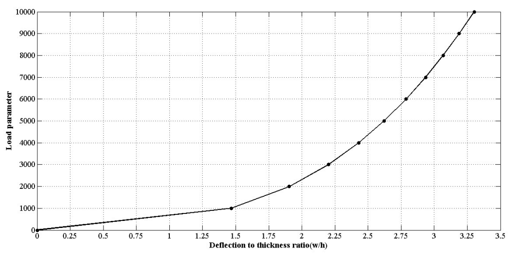


**Fig. 26.** The load- maximum deflection curves for the circular plate with a rectangular opening

### 3.13 The L-shaped plate with opening

Here, the plate shown in Fig. 27 is studied. Values of **a** and **b** are 0.3 and 0.2 m, respectively. The maximum deflection occurs at a node with coordinates (1.4, 0.5) m. This structure is modeled by 199 bending elements. The results are shown in

**Tab. 19.** The ranking of methods for the plate with arched edges

| Method | Number of iterations in each loading step | | | | | | | | | | Total Iterations | Score | Grade | Time (Second) | Score | Grade |
|---|---|---|---|---|---|---|---|---|---|---|---|---|---|---|---|---|
| | 1 | 2 | 3 | 4 | 5 | 6 | 7 | 8 | 9 | 10 | | | | | | |
| 1 | 14501 | 11512 | 10540 | 12149 | 8791 | 10330 | 8367 | 7959 | 9168 | 6890 | 100207 | 0 | 14 | 21430.75 | 0 | 14 |
| 2 | 1260 | 1052 | 962 | 903 | 834 | 810 | 781 | 760 | 763 | 639 | 8764 | 100 | 1 | 1385.687 | 100 | 1 |
| 3 | 1566 | 1352 | 1246 | 1170 | 1112 | 1065 | 1027 | 995 | 967 | 943 | 11443 | 97.07 | 9 | 2186.328 | 96.006 | 10 |
| 4 | 1208 | 1051 | 986 | 925 | 894 | 865 | 837 | 808 | 790 | 769 | 9133 | 99.596 | 2 | 1443.141 | 99.713 | 2 |
| 5 | 1267 | 1101 | 1035 | 971 | 939 | 906 | 878 | 849 | 828 | 804 | 9578 | 99.11 | 6 | 1512.156 | 99.369 | 4 |
| 6 | 1996 | 1735 | 1656 | 1218 | 1189 | 1136 | 1086 | 1067 | 1031 | 1017 | 13131 | 95.224 | 12 | 2063.937 | 96.616 | 8 |
| 7 | Fail | Fail | Fail | Fail | Fail | Fail | Fail | Fail | Fail | Fail | | | 0 | | | 0 |
| 8 | 1768 | 1703 | 1477 | 1356 | 1245 | 1229 | 1114 | 1089 | 1069 | 1060 | 13110 | 95.247 | 11 | 2180.641 | 96.034 | 9 |
| 9 | 1281 | 1101 | 1035 | 971 | 939 | 906 | 878 | 849 | 828 | 804 | 9592 | 99.095 | 7 | 1942.312 | 97.223 | 7 |
| 10 | 1208 | 1049 | 986 | 929 | 894 | 865 | 837 | 808 | 789 | 769 | 9134 | 99.595 | 3 | 1468.672 | 99.586 | 3 |
| 11 | 1597 | 1016 | 986 | 929 | 894 | 864 | 837 | 808 | 789 | 769 | 9489 | 99.207 | 5 | 1917.828 | 97.345 | 6 |
| 12 | 1427 | 1012 | 986 | 929 | 894 | 864 | 837 | 808 | 789 | 769 | 9315 | 99.397 | 4 | 1887.047 | 97.499 | 5 |
| 13 | 1566 | 1352 | 1245 | 1169 | 1111 | 1065 | 1027 | 995 | 967 | 942 | 11439 | 97.075 | 8 | 3327.14 | 90.315 | 12 |
| 14 | 1584 | 1368 | 1262 | 1186 | 1129 | 1083 | 1045 | 1013 | 985 | 961 | 11616 | 96.881 | 10 | 3390.437 | 89.999 | 13 |
| 15 | 1732 | 1773 | 1791 | 1806 | 1811 | 1821 | 1829 | 1839 | 1833 | 1851 | 18086 | 89.806 | 13 | 2838.125 | 92.754 | 11 |
| 16 | Fail | Fail | Fail | Fail | Fail | Fail | Fail | Fail | Fail | Fail | | | 0 | | | 0 |

**Tab. 20.** The ranking of methods for the circular plate with rectangular opening

| Method | Number of iterations in each loading step | | | | | | | | | | Total Iterations | Score | Grade | Time (Second) | Score | Grade |
|---|---|---|---|---|---|---|---|---|---|---|---|---|---|---|---|---|
| | 1 | 2 | 3 | 4 | 5 | 6 | 7 | 8 | 9 | 10 | | | | | | |
| 1 | 3285 | 4630 | 4162 | 4122 | 5389 | 2329 | 1627 | 2489 | 2451 | 2735 | 33219 | 0 | 14 | 2314.219 | 0 | 14 |
| 2 | 590 | 552 | 465 | 460 | 483 | 421 | 389 | 426 | 410 | 409 | 4605 | 100 | 1 | 277.469 | 100 | 1 |
| 3 | 693 | 630 | 594 | 568 | 548 | 533 | 521 | 512 | 504 | 498 | 5601 | 96.519 | 10 | 358.25 | 96.034 | 9 |
| 4 | 568 | 539 | 528 | 502 | 496 | 483 | 471 | 459 | 450 | 443 | 4939 | 98.833 | 3 | 296.797 | 99.051 | 3 |
| 5 | 595 | 566 | 551 | 527 | 520 | 507 | 494 | 481 | 471 | 460 | 5172 | 98.018 | 5 | 311.141 | 98.347 | 5 |
| 6 | 621 | 552 | 510 | 518 | 497 | 479 | 460 | 450 | 465 | 457 | 5009 | 98.588 | 4 | 301.516 | 98.819 | 4 |
| 7 | Fail | Fail | Fail | Fail | Fail | Fail | Fail | Fail | Fail | Fail | | | 0 | | | 0 |
| 8 | 920 | 899 | 846 | 753 | 785 | 708 | 692 | 682 | 689 | 675 | 7649 | 89.362 | 12 | 509.688 | 88.599 | 12 |
| 9 | 608 | 565 | 551 | 527 | 520 | 507 | 494 | 481 | 471 | 460 | 5184 | 97.977 | 6 | 342.078 | 96.828 | 6 |
| 10 | 567 | 539 | 524 | 503 | 495 | 483 | 471 | 459 | 450 | 438 | 4929 | 98.868 | 2 | 296.688 | 99.056 | 2 |
| 11 | 814 | 561 | 524 | 501 | 495 | 483 | 471 | 459 | 450 | 438 | 5196 | 97.935 | 7 | 344.031 | 96.732 | 7 |
| 12 | 814 | 561 | 527 | 501 | 495 | 483 | 471 | 459 | 450 | 438 | 5199 | 97.924 | 8 | 344.266 | 96.72 | 8 |
| 13 | 693 | 630 | 594 | 568 | 548 | 533 | 521 | 511 | 504 | 498 | 5600 | 96.523 | 9 | 425.719 | 92.721 | 10 |
| 14 | 709 | 644 | 608 | 582 | 563 | 548 | 536 | 527 | 520 | 514 | 5751 | 95.995 | 11 | 435.14 | 92.259 | 11 |
| 15 | 889 | 937 | 967 | 982 | 1001 | 1009 | 1027 | 1041 | 1052 | 1048 | 9953 | 81.31 | 13 | 599.344 | 84.197 | 13 |
| 16 | Fail | Fail | Fail | Fail | Fail | Fail | Fail | Fail | Fail | Fail | | | 0 | | | 0 |

Fig. 28. The ranking and scores of the methods are illustrated in Table 21. Both RPTH schemes are divergent. For this reason, the rank of these tactics is zero. Moreover, the MRE and mdDR2 processes have obtained the first rank from the point of view of the number of iterations. On the other hand, Zhang1 technique has the first rank considering the analysis time.

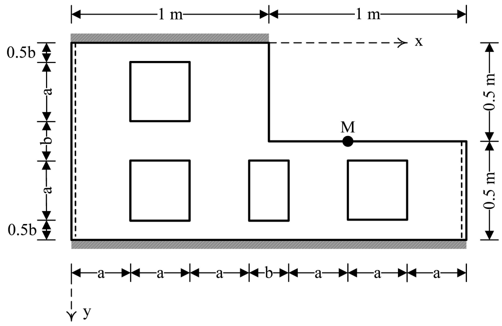


**Fig. 27.** The L-shaped plate with opening

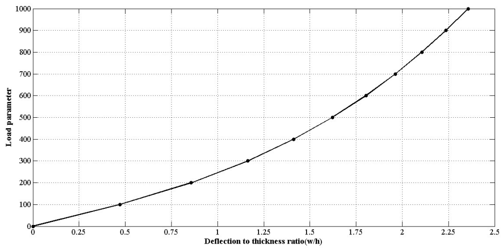


**Fig. 28.** The load- maximum deflection curves for the L-shaped plate with opening

### 3.14 The rectangular plate with the circular hole

In this section, the quadrilateral plate of Fig. 29 is analyzed. One-quarter of the structure is modeled with 76 elements. The results are shown in Fig. 30 and inserted in Table 22. According to Table 22, RPTH1 and RPTH2 algorithms are not able to find the responses. Moreover, Zhang1 and mdDR1 approaches had the same behavior. These two strategies provide the best solution for this plate. Moreover, Papadrakakis tactic is the worst one.

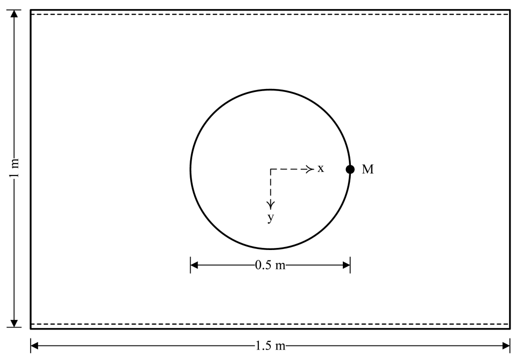


**Fig. 29.** The rectangular plate with circular hole

### 3.15 The sector donut

In this example, the structure shown in Fig. 31 is solved by using 90 elements. The maximum deflection occurs in the middle

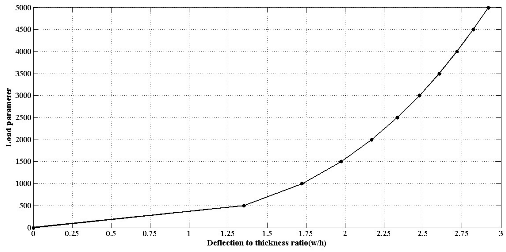


**Fig. 30.** The load- maximum deflection curves for the rectangular plate with the circular hole

of the inner edge. Fig. 32 demonstrates the load-displacement curve for this node. The number of iterations and the time taken for the analysis are inserted in Table 23. In this problem, Underwood method holds the first rank.

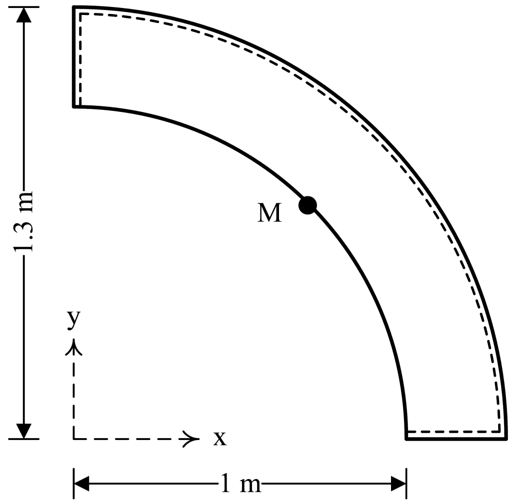


**Fig. 31.** The sector donut

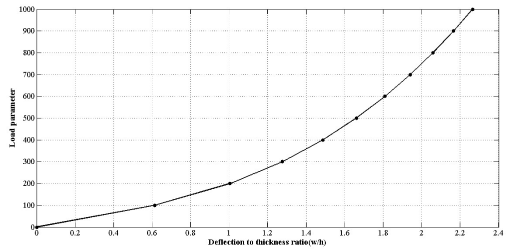


**Fig. 32.** The load- maximum deflection curves for the sector donut

### 3.16 The sector plate

The final sample is a quarter of a circular plate. Fig. 33 shows the geometry of this structure. Its finite element meshing is done by utilizing 113 bending elements. The maximum deflection is at the central node of the outer boundary. The results are presented in Fig. 34. Table 24 lists the ranking of procedures. RPTH1, RPTH2 and MFT approaches were not able to solve this plate. Moreover, Underwood technique is the best tactic to find the solution for this problem.

## 4 The ranking of methods

Based on the number of iterations and the required time for the analysis, the rank of each method in each sample was

**Tab. 21.** The ranking of methods for the L-shaped plate with opening

| Method | Number of iterations in each loading step | | | | | | | | | | Total Iterations | Score | Grade | Time (Second) | Score | Grade |
|---|---|---|---|---|---|---|---|---|---|---|---|---|---|---|---|---|
| | 1 | 2 | 3 | 4 | 5 | 6 | 7 | 8 | 9 | 10 | | | | | | |
| 1 | 13799 | 9244 | 13535 | 24567 | 16894 | 11845 | 9314 | 8244 | 7222 | 12870 | 127534 | 0 | 13 | 6156.813 | 0 | 14 |
| 2 | 1626 | 1492 | 1218 | 1156 | 1119 | 1178 | 1100 | 1095 | 898 | 1084 | 11966 | 98.734 | 6 | 515.671 | 98.869 | 6 |
| 3 | 3510 | 2956 | 2791 | 2683 | 2602 | 2537 | 2483 | 2438 | 2398 | 2362 | 26760 | 86.095 | 11 | 1223.234 | 86.468 | 11 |
| 4 | 1408 | 1281 | 1154 | 1092 | 1007 | 976 | 935 | 900 | 884 | 848 | 10485 | 99.999 | 2 | 451.125 | 100 | 1 |
| 5 | 1476 | 1347 | 1211 | 1146 | 1063 | 1024 | 975 | 945 | 920 | 890 | 10997 | 99.562 | 4 | 473.719 | 99.604 | 3 |
| 6 | 2385 | 1770 | 1613 | 1518 | 1446 | 1391 | 1346 | 1310 | 1279 | 1252 | 15310 | 95.877 | 8 | 661.656 | 96.31 | 9 |
| 7 | Fail | Fail | Fail | Fail | Fail | Fail | Fail | Fail | Fail | Fail | | | 0 | | | 0 |
| 8 | 2221 | 2169 | 1854 | 1740 | 1557 | 1467 | 1424 | 1530 | 1372 | 1430 | 16764 | 94.635 | 9 | 754.922 | 94.676 | 10 |
| 9 | 1686 | 1350 | 1211 | 1140 | 1063 | 1024 | 975 | 945 | 920 | 890 | 11204 | 99.385 | 5 | 527.109 | 98.668 | 7 |
| 10 | 1407 | 1281 | 1154 | 1092 | 1007 | 976 | 935 | 900 | 884 | 848 | 10484 | 100 | 1 | 452.078 | 99.983 | 2 |
| 11 | 1617 | 1281 | 1154 | 1092 | 1007 | 976 | 935 | 900 | 884 | 848 | 10694 | 99.821 | 3 | 503.063 | 99.09 | 5 |
| 12 | 1617 | 1281 | 1154 | 1092 | 1007 | 976 | 935 | 900 | 884 | 848 | 10694 | 99.821 | 3 | 503.047 | 99.09 | 4 |
| 13 | 3510 | 2956 | 2791 | 2683 | 2602 | 2537 | 2483 | 2437 | 2397 | 2362 | 26758 | 86.097 | 10 | 1377.844 | 83.758 | 12 |
| 14 | 3550 | 2994 | 2832 | 2726 | 2646 | 2582 | 2529 | 2484 | 2445 | 2410 | 27198 | 85.721 | 12 | 1426.109 | 82.912 | 13 |
| 15 | 2894 | 1684 | 1103 | 1031 | 1007 | 1029 | 1025 | 1028 | 1032 | 1046 | 12879 | 97.954 | 7 | 553.485 | 98.206 | 8 |
| 16 | Fail | Fail | Fail | Fail | Fail | Fail | Fail | Fail | Fail | Fail | | | 0 | | | 0 |

**Tab. 22.** The ranking of methods for the rectangular plate with the circular hole

| Method | Number of iterations in each loading step | | | | | | | | | | Total Iterations | Score | Grade | Time (Second) | Score | Grade |
|---|---|---|---|---|---|---|---|---|---|---|---|---|---|---|---|---|
| | 1 | 2 | 3 | 4 | 5 | 6 | 7 | 8 | 9 | 10 | | | | | | |
| 1 | 17362 | 17257 | 14189 | 7727 | 6789 | 7717 | 6612 | 6460 | 5516 | 5360 | 94989 | 0 | 12 | 5881.203 | 0 | 14 |
| 2 | 1313 | 1356 | 1284 | 1082 | 1089 | 1041 | 1060 | 970 | 1002 | 961 | 11158 | 100 | 1 | 573.125 | 100 | 1 |
| 3 | 2846 | 3127 | 3108 | 3035 | 2959 | 2891 | 2831 | 2778 | 2731 | 2689 | 28995 | 78.723 | 10 | 1601.782 | 80.621 | 11 |
| 4 | 1166 | 1363 | 1336 | 1270 | 1225 | 1210 | 1196 | 1181 | 1140 | 1119 | 12206 | 98.75 | 2 | 626 | 99.004 | 2 |
| 5 | 1223 | 1424 | 1404 | 1326 | 1279 | 1270 | 1255 | 1235 | 1194 | 1174 | 12784 | 98.06 | 4 | 655.844 | 98.442 | 4 |
| 6 | 1588 | 1446 | 1318 | 1356 | 1293 | 1249 | 1195 | 1165 | 1123 | 1098 | 12831 | 98.004 | 5 | 658.984 | 98.382 | 5 |
| 7 | Fail | Fail | Fail | Fail | Fail | Fail | Fail | Fail | Fail | Fail | | | 0 | | | 0 |
| 8 | 1878 | 1792 | 1637 | 1767 | 1740 | 1539 | 1532 | 1582 | 1447 | 1242 | 16156 | 94.038 | 8 | 867.172 | 94.46 | 10 |
| 9 | 1610 | 1424 | 1404 | 1326 | 1279 | 1270 | 1255 | 1235 | 1194 | 1174 | 13171 | 97.599 | 6 | 755.516 | 96.564 | 9 |
| 10 | 1166 | 1362 | 1337 | 1268 | 1225 | 1210 | 1197 | 1181 | 1140 | 1120 | 12206 | 98.75 | 2 | 627.234 | 98.981 | 3 |
| 11 | 1454 | 1362 | 1337 | 1268 | 1225 | 1210 | 1197 | 1181 | 1140 | 1119 | 12493 | 98.408 | 3 | 717.422 | 97.282 | 7 |
| 12 | 1454 | 1362 | 1337 | 1268 | 1225 | 1210 | 1197 | 1181 | 1140 | 1119 | 12493 | 98.408 | 3 | 720.843 | 97.217 | 8 |
| 13 | 2846 | 3127 | 3108 | 3034 | 2959 | 2890 | 2830 | 2777 | 2730 | 2689 | 28990 | 78.729 | 9 | 1969.406 | 73.695 | 12 |
| 14 | 2874 | 3164 | 3151 | 3081 | 3008 | 2941 | 2882 | 2830 | 2785 | 2744 | 29460 | 78.168 | 11 | 1999.375 | 73.131 | 13 |
| 15 | 3058 | 2050 | 1408 | 1022 | 1023 | 1052 | 1041 | 1070 | 1055 | 1099 | 13878 | 96.755 | 7 | 711.765 | 97.388 | 6 |
| 16 | Fail | Fail | Fail | Fail | Fail | Fail | Fail | Fail | Fail | Fail | | | 0 | | | 0 |

**Tab. 23.** The ranking of methods for the sector donut

| Method | Number of iterations in each loading step | | | | | | | | | | Total Iterations | Score | Grade | Time (Second) | Score | Grade |
|---|---|---|---|---|---|---|---|---|---|---|---|---|---|---|---|---|
| | 1 | 2 | 3 | 4 | 5 | 6 | 7 | 8 | 9 | 10 | | | | | | |
| 1 | 7352 | 10009 | 9798 | 5434 | 7229 | 8374 | 6113 | 17509 | 6242 | 5213 | 83273 | 0 | 12 | 6733.235 | 0 | 13 |
| 2 | 1296 | 1106 | 1296 | 1027 | 1051 | 1161 | 1149 | 1139 | 1027 | 1018 | 11270 | 100 | 1 | 748.234 | 100 | 1 |
| 3 | 3472 | 3189 | 3090 | 3032 | 2995 | 2970 | 2953 | 2941 | 2933 | 2928 | 30503 | 73.289 | 10 | 2243.969 | 75.009 | 10 |
| 4 | 1724 | 1442 | 1328 | 1275 | 1223 | 1192 | 1162 | 1121 | 1094 | 1075 | 12636 | 98.103 | 2 | 841.375 | 98.444 | 2 |
| 5 | 1808 | 1512 | 1393 | 1335 | 1282 | 1250 | 1219 | 1175 | 1147 | 1125 | 13246 | 97.256 | 5 | 882.563 | 97.756 | 4 |
| 6 | 2087 | 1629 | 1529 | 1449 | 1309 | 1279 | 1256 | 1239 | 1219 | 1203 | 14199 | 95.932 | 6 | 950.766 | 96.616 | 5 |
| 7 | Fail | Fail | Fail | Fail | Fail | Fail | Fail | Fail | Fail | Fail | | | 0 | | | 0 |
| 8 | 2645 | 2000 | 1832 | 1635 | 1764 | 1609 | 1542 | 1659 | 1562 | 1545 | 17793 | 90.941 | 8 | 1240.703 | 91.772 | 9 |
| 9 | Fail | Fail | Fail | Fail | Fail | Fail | Fail | Fail | Fail | Fail | | | 0 | | | 0 |
| 10 | 1724 | 1442 | 1330 | 1275 | 1222 | 1192 | 1162 | 1121 | 1095 | 1075 | 12638 | 98.1 | 3 | 846.953 | 98.351 | 3 |
| 11 | 1739 | 1442 | 1330 | 1277 | 1222 | 1192 | 1162 | 1121 | 1095 | 1075 | 12655 | 98.076 | 4 | 978.125 | 96.159 | 7 |
| 12 | 1739 | 1442 | 1330 | 1277 | 1222 | 1192 | 1162 | 1121 | 1095 | 1075 | 12655 | 98.076 | 4 | 980.828 | 96.114 | 8 |
| 13 | 3471 | 3189 | 3089 | 3031 | 2994 | 2969 | 2952 | 2940 | 2932 | 2927 | 30494 | 73.301 | 9 | 2873.031 | 64.498 | 11 |
| 14 | 3522 | 3240 | 3143 | 3087 | 3052 | 3028 | 3013 | 3002 | 2996 | 2992 | 31075 | 72.494 | 11 | 2946.594 | 63.269 | 12 |
| 15 | 1349 | 1409 | 1425 | 1462 | 1472 | 1467 | 1510 | 1513 | 1514 | 1516 | 14637 | 95.324 | 7 | 976.141 | 96.192 | 6 |
| 16 | Fail | Fail | Fail | Fail | Fail | Fail | Fail | Fail | Fail | Fail | | | 0 | | | 0 |

**Tab. 24.** The ranking of methods for the sector plate

| Method | Number of iterations in each loading step | | | | | | | | | | Total Iterations | Score | Grade | Time (Second) | Score | Grade |
|---|---|---|---|---|---|---|---|---|---|---|---|---|---|---|---|---|
| | 1 | 2 | 3 | 4 | 5 | 6 | 7 | 8 | 9 | 10 | | | | | | |
| 1 | 2232 | 1736 | 2335 | 2513 | 2471 | 2621 | 2119 | 2097 | 3604 | 2781 | 24509 | 0 | 14 | 813.672 | 0 | 14 |
| 2 | 374 | 302 | 286 | 246 | 262 | 235 | 212 | 220 | 231 | 223 | 2591 | 100 | 1 | 83.328 | 100 | 1 |
| 3 | 382 | 336 | 317 | 305 | 298 | 293 | 291 | 290 | 289 | 290 | 3091 | 97.719 | 9 | 102.469 | 97.379 | 7 |
| 4 | 344 | 329 | 313 | 296 | 285 | 278 | 271 | 264 | 259 | 255 | 2894 | 98.618 | 3 | 93.078 | 98.665 | 3 |
| 5 | 361 | 346 | 326 | 310 | 299 | 292 | 284 | 277 | 271 | 267 | 3033 | 97.983 | 6 | 97.297 | 98.087 | 4 |
| 6 | 521 | 546 | 537 | 526 | 515 | 503 | 490 | 477 | 476 | 461 | 5052 | 88.772 | 12 | 162.188 | 89.202 | 11 |
| 7 | Fail | Fail | Fail | Fail | Fail | Fail | Fail | Fail | Fail | Fail | | | 0 | | | 0 |
| 8 | 588 | 518 | 449 | 461 | 461 | 450 | 416 | 426 | 395 | 420 | 4584 | 90.907 | 11 | 173.75 | 87.619 | 12 |
| 9 | 375 | 343 | 325 | 308 | 299 | 289 | 284 | 277 | 271 | 267 | 3038 | 97.961 | 7 | 103.047 | 97.3 | 8 |
| 10 | 344 | 329 | 310 | 296 | 288 | 278 | 270 | 264 | 258 | 255 | 2892 | 98.627 | 2 | 92.796 | 98.704 | 2 |
| 11 | 357 | 329 | 310 | 296 | 288 | 278 | 270 | 264 | 258 | 255 | 2905 | 98.567 | 4 | 98.188 | 97.965 | 5 |
| 12 | 365 | 329 | 310 | 296 | 288 | 278 | 270 | 264 | 258 | 255 | 2913 | 98.531 | 5 | 98.657 | 97.901 | 6 |
| 13 | 382 | 336 | 316 | 305 | 297 | 293 | 291 | 289 | 289 | 289 | 3087 | 97.737 | 8 | 106.516 | 96.825 | 9 |
| 14 | 397 | 350 | 331 | 319 | 313 | 309 | 307 | 306 | 306 | 307 | 3245 | 97.016 | 10 | 111.141 | 96.192 | 10 |
| 15 | 713 | 758 | 778 | 799 | 812 | 823 | 834 | 848 | 853 | 857 | 8075 | 74.979 | 13 | 257.641 | 76.133 | 13 |
| 16 | Fail | Fail | Fail | Fail | Fail | Fail | Fail | Fail | Fail | Fail | | | 0 | | | 0 |

**Tab. 25.** The ranking of methods based on the number of iteration

| Grade | Score ($S_i$) | Method | $Q_{ij}$ | | | | | | | | | | | | | | | | |
|---|---|---|---|---|---|---|---|---|---|---|---|---|---|---|---|---|---|---|---|
| | | | 0 | 1 | 2 | 3 | 4 | 5 | 6 | 7 | 8 | 9 | 10 | 11 | 12 | 13 | 14 | 15 | 16 |
| 1 | 94.5652 | 2 | 0 | 17 | 0 | 2 | 2 | 0 | 2 | 0 | 0 | 0 | 0 | 0 | 0 | 0 | 0 | 0 | 0 |
| 2 | 84.5109 | 10 | 0 | 1 | 9 | 3 | 2 | 6 | 0 | 2 | 0 | 0 | 0 | 0 | 0 | 0 | 0 | 0 | 0 |
| 3 | 83.6957 | 4 | 0 | 1 | 5 | 8 | 3 | 2 | 3 | 0 | 1 | 0 | 0 | 0 | 0 | 0 | 0 | 0 | 0 |
| 4 | 76.087 | 11 | 0 | 2 | 1 | 3 | 5 | 2 | 5 | 2 | 3 | 0 | 0 | 0 | 0 | 0 | 0 | 0 | 0 |
| 5 | 68.75 | 12 | 2 | 2 | 0 | 3 | 5 | 3 | 2 | 3 | 2 | 1 | 0 | 0 | 0 | 0 | 0 | 0 | 0 |
| 6 | 60.0543 | 5 | 0 | 0 | 0 | 0 | 2 | 5 | 3 | 4 | 1 | 3 | 2 | 1 | 1 | 1 | 0 | 0 | 0 |
| 7 | 58.6957 | 13 | 0 | 0 | 5 | 0 | 0 | 0 | 1 | 1 | 2 | 7 | 4 | 3 | 0 | 0 | 0 | 0 | 0 |
| 8 | 55.9783 | 6 | 0 | 0 | 0 | 0 | 1 | 3 | 3 | 3 | 5 | 2 | 2 | 0 | 3 | 1 | 0 | 0 | 0 |
| 9 | 55.163 | 9 | 2 | 0 | 0 | 1 | 1 | 2 | 5 | 3 | 3 | 2 | 1 | 2 | 1 | 0 | 0 | 0 | 0 |
| 10 | 52.9891 | 3 | 0 | 0 | 1 | 4 | 0 | 0 | 0 | 1 | 1 | 2 | 8 | 3 | 3 | 0 | 0 | 0 | 0 |
| 11 | 45.6522 | 14 | 0 | 0 | 0 | 1 | 4 | 0 | 0 | 0 | 1 | 0 | 2 | 8 | 3 | 4 | 0 | 0 | 0 |
| 12 | 43.2065 | 8 | 0 | 0 | 1 | 0 | 0 | 0 | 0 | 0 | 6 | 4 | 1 | 5 | 2 | 0 | 3 | 1 | 0 |
| 13 | 42.1196 | 15 | 0 | 0 | 0 | 0 | 2 | 1 | 0 | 5 | 0 | 1 | 2 | 0 | 4 | 4 | 1 | 3 | 0 |
| 14 | 23.0978 | 1 | 0 | 0 | 0 | 0 | 0 | 0 | 0 | 0 | 0 | 0 | 1 | 1 | 5 | 7 | 5 | 0 | 4 |
| 15 | 14.6739 | 16 | 19 | 2 | 0 | 1 | 0 | 0 | 0 | 0 | 0 | 1 | 0 | 0 | 0 | 0 | 0 | 0 | 0 |
| 16 | 14.1304 | 7 | 19 | 0 | 3 | 0 | 0 | 0 | 0 | 0 | 0 | 0 | 1 | 0 | 0 | 0 | 0 | 0 | 0 |

**Tab. 26.** The ranking of methods based on the analysis time

| Grade | Score ($S_i$) | Method | $Q_{ij}$ | | | | | | | | | | | | | | | | |
|---|---|---|---|---|---|---|---|---|---|---|---|---|---|---|---|---|---|---|---|
| | | | 0 | 1 | 2 | 3 | 4 | 5 | 6 | 7 | 8 | 9 | 10 | 11 | 12 | 13 | 14 | 15 | 16 |
| 1 | 95.1087 | 2 | 0 | 17 | 0 | 3 | 1 | 1 | 1 | 0 | 0 | 0 | 0 | 0 | 0 | 0 | 0 | 0 | 0 |
| 2 | 88.0435 | 4 | 0 | 2 | 9 | 5 | 5 | 1 | 0 | 1 | 0 | 0 | 0 | 0 | 0 | 0 | 0 | 0 | 0 |
| 3 | 86.413 | 10 | 0 | 2 | 6 | 9 | 1 | 4 | 0 | 0 | 1 | 0 | 0 | 0 | 0 | 0 | 0 | 0 | 0 |
| 4 | 71.4674 | 5 | 0 | 0 | 0 | 2 | 8 | 3 | 4 | 2 | 1 | 2 | 0 | 1 | 0 | 0 | 0 | 0 | 0 |
| 5 | 65.7609 | 6 | 0 | 0 | 1 | 0 | 2 | 7 | 6 | 0 | 1 | 3 | 0 | 3 | 0 | 0 | 0 | 0 | 0 |
| 6 | 62.2283 | 11 | 0 | 0 | 0 | 0 | 1 | 3 | 5 | 8 | 1 | 3 | 0 | 2 | 0 | 0 | 0 | 0 | 0 |
| 7 | 53.2609 | 3 | 0 | 0 | 3 | 0 | 1 | 0 | 1 | 2 | 0 | 3 | 5 | 8 | 0 | 0 | 0 | 0 | 0 |
| 8 | 51.6304 | 12 | 2 | 0 | 0 | 0 | 1 | 1 | 1 | 4 | 9 | 1 | 2 | 1 | 1 | 0 | 0 | 0 | 0 |
| 9 | 46.4674 | 9 | 2 | 0 | 0 | 1 | 0 | 0 | 1 | 3 | 5 | 3 | 4 | 1 | 1 | 2 | 0 | 0 | 0 |
| 10 | 45.9239 | 15 | 0 | 0 | 0 | 0 | 2 | 3 | 2 | 1 | 2 | 0 | 1 | 2 | 3 | 4 | 1 | 2 | 0 |
| 11 | 42.9348 | 8 | 0 | 0 | 1 | 0 | 0 | 0 | 1 | 0 | 0 | 7 | 5 | 0 | 7 | 1 | 0 | 1 | 0 |
| 12 | 40.4891 | 13 | 0 | 0 | 0 | 2 | 0 | 0 | 0 | 1 | 1 | 1 | 4 | 1 | 9 | 3 | 1 | 0 | 0 |
| 13 | 32.337 | 14 | 0 | 0 | 0 | 0 | 0 | 0 | 1 | 1 | 1 | 0 | 1 | 4 | 2 | 10 | 2 | 1 | 0 |
| 14 | 18.4783 | 1 | 0 | 0 | 0 | 0 | 0 | 0 | 0 | 0 | 0 | 0 | 1 | 0 | 0 | 3 | 15 | 0 | 4 |
| 15 | 16.3043 | 16 | 19 | 2 | 1 | 0 | 1 | 0 | 0 | 0 | 0 | 0 | 0 | 0 | 0 | 0 | 0 | 0 | 0 |
| 16 | 14.1304 | 7 | 19 | 0 | 2 | 1 | 0 | 0 | 0 | 0 | 0 | 1 | 0 | 0 | 0 | 0 | 0 | 0 | 0 |

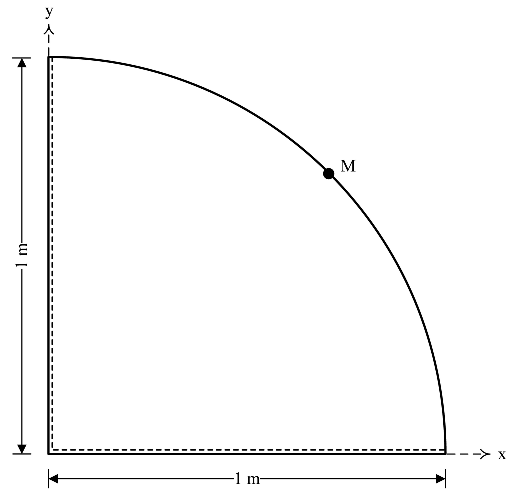


**Fig. 33.** The sector plate

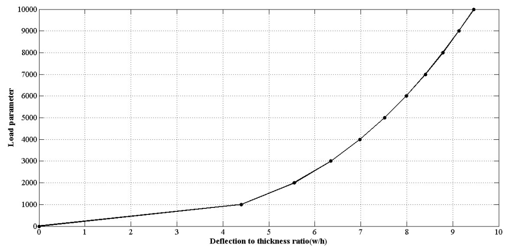


**Fig. 34.** The load- maximum deflection curves for the sector plate

achieved. Rank number one indicates the best process and rank number sixteen indicates the worst approach. Here, the ***j-th*** rank of the ***i-th*** scheme is shown by $Q_{ij}$. For example, Underwood solution has ranked first for seventeen times. So, $Q_{i1}$ for this tactic is seventeen. $Q_{i0}$ is the number of structures that the approach $i$ has not been able to analyze. The rating of algorithm $i$ is obtained using Eq. (48). It is worth emphasizing; if the procedure is not able to reach the proper response, then it is not entered into the Eq. (48):

$$S_i = 100 \times \sum_{j=1}^{16} Q_{ij} \times (17 - j)/368 \tag{48}$$

It should be noted that if a technique has acquired the number of 368, then that strategy has first rank in all 23 numerical samples. As a result, the rating $S_i$ will be 100 for that solution. The rating and the final ranking of each method are shown in Tables 25 and 26.

## 5 Conclusion

In this paper, sixteen well-known dynamic relaxation methods were used for solving bending plate. First, the basis of dynamic relaxation approach and the related relationships were presented. Then, the previous procedures reviewed for estimating the fictitious parameters needed for each technique. Afterwards, several bending plate samples with geometrically nonlinear behavior were analyzed. The criteria chosen were the number of iterations and total analysis time. On this basis, various processes were ranked. The results of this study revealed that Underwood solution took the lowest number of iterations to give the answer. Moreover, Zhang1 and mdDR1 tactics occupy the next-best subsequent ranks. Moreover, these procedures are the best techniques from the point of view analysis time. Rezaiee-Pajand and Taghavian Hakkak scheme was the worst strategy due to the usage of second-order approximations. Because, this process diverged in 19 examples. Among the methods that converged, Papadrakakis algorithm needed the largest number of iterations and the longest time to reach the assumed accuracy. In most samples, the MRE and mdDR2 processes as well as Qiang and RPS approaches had a similar behavior. Such features were also true for Zhang1 and mdDR1 as well as the MFT and Zhang2 techniques. In other words, the number of iterations required to run these procedures were almost the same.

## References

1 **Szilard R**, *Theories and applications of plate analysis: classical numerical and engineering methods*, John Wiley & Sons; New Jersey, USA, 2004.

2 **Levy S**, *Bending of rectangular plates with large deflections*, NACA Technical Note 846, (1942), 1-46.

3 **Bergan PG, Clough RW**, *Large deflection analysis of plates and shallow shells using the finite element method*, International Journal for Numerical Methods in Engineering, **5**(4), (1973), 543-556, DOI 10.1002/nme.1620050410.

4 **Yang R, Bhatti M**, *Nonlinear static and dynamic analysis of plates*, Journal of Engineering Mechanics, **111**(2), (1985), 175-187, DOI 10.1061/(ASCE)0733-9399(1985)111:2(175).

5 **Rushton KR**, *Large deflecion of variable-thickness plates*, International Journal of Mechanical Sciences, **10**(9), (1968), 723-735, DOI 10.1016/0020-7403(68)90086-6.

6 **Rushton KR**, *Postbuckling of tapered plates*, International Journal of Mechanical Sciences, **11**(5), (1969), 461-480, DOI 10.1016/0020-7403(69)90031-9.

7 **Basu A, Dawson J**, *Orthotropic sandwich plates*, In: Inst Civil Engineers Proc; London, UK, 1970, pp. 87-115.

8 **Rushton KR**, *Buckling of laterally loaded plates having initial curvature*, International Journal of Mechanical Sciences, **14**(10), (1972), 667-680, DOI 10.1016/0020-7403(72)90024-0.

9 **Turvey G, Wittrick W**, *The large deflection and post-buckling behaviour of some laminated plates*, Aeronautical Quarterly, **24**, (1973), 77-86.

10 **Alwar RS, Rao NR**, *Nonlinear analysis of orthotropic skew plates*, AIAA Journal, **11**(4), (1973), 495-498, DOI 10.2514/3.6777.

11 **Alwar RS, Rao NR**, *Large elastic deformations of clamped skewed plates by dynamic relaxation*, Computers & Structures, **4**(2), (1974), 381-398, DOI 10.1016/0045-7949(74)90065-0.

12 **Rushton KR, Hook PM**, *Large deflection of plates and beams obeying nonlinear stress – strain laws*, The Journal of Strain Analysis for Engineering Design, **9**(3), (1974), 178-184.

13 **Hook PM, Rushton KR**, *Buckling of beams and plates onto an intermediate support studied by the dynamic relaxation method*, The Journal of Strain Analysis for Engineering Design, **10**(3), (1975), 153-158, DOI 10.1243/03093247V103153.

14 **Frieze PA, Hobbs RE, Dowling PJ**, *Application of dynamic relaxation to the large deflection elasto-plastic analysis of plates*, Computers & Structures, **8**(2), (1978), 301-310, DOI 10.1016/0045-7949(78)90037-8.

15 **Turvey GJ**, *Large deflection of tapered annular plates by dynamic relaxation*, Journal of the Engineering Mechanics Division, **104**(2), (1978), 351-366.

16 **Pica A, Hinton E**, *Transient and pseudo-transient analysis of Mindlin plates*,

International Journal for Numerical Methods in Engineering, **15**(2), (1980), 189-208, DOI 10.1002/nme.1620150204.

17 **Al-Shawi FAN, Mardirosian AH**, *An improved dynamic relaxation method for the analysis of plate bending problems*, Computers & Structures, **27**(2), (1987), 237-240, DOI 10.1016/0045-7949(87)90091-5.

18 **Zhang LG, Yu TX**, *Modified adaptive dynamic relaxation method and its application to elastic-plastic bending and wrinkling of circular plates*, Computers & Structures, **33**(2), (1989), 609-614, DOI 10.1016/0045-7949(89)90035-7.

19 **Turvey GJ, Osman MY**, *Elastic large deflection analysis of isotropic rectangular Mindlin plates*, International Journal of Mechanical Sciences, **32**(4), (1990), 315-328, DOI 10.1016/0020-7403(90)90096-2.

20 **Turvey GJ, Salehi M**, *DR large deflection analysis of sector plates*, Computers & Structures, **34**(1), (1990), 101-112, DOI 10.1016/0045-7949(90)90304-K.

21 **Salehi M, Turvey GJ**, *Elastic large deflection response of annular sector plates – a comparison of dr finite-difference, finite element and other numerical solutions*, Computers & Structures, **40**(5), (1991), 1267-1278, DOI 10.1016/0045-7949(91)90397-5.

22 **Kadkhodayan M, Zhang LC, Sowerby R**, *Analyses of wrinkling and buckling of elastic plates by DXDR method*, Computers & Structures, **65**(4), (1997), 561-574, DOI 10.1016/S0045-7949(96)00368-9.

23 **Turvey GJ, Salehi M**, *Annular sector plates: Comparison of full-section and layer yield predictions*, Computers & Structures, **83**(28 – 30), (2005), 2431-2441, DOI 10.1016/j.compstruc.2005.03.025.

24 **Salehi M, Aghaei H**, *Dynamic relaxation large deflection analysis of non-axisymmetric circular viscoelastic plates*, Computers & Structures, **83**(23-24), (2005), 1878-1890, DOI 10.1016/j.compstruc.2005.02.023.

25 **Falahatgar SR, Salehi M**, *Dynamic relaxation nonlinear viscoelastic bending analysis of higher-order annular sector plates*, International Journal for Computational Methods in Engineering Science and Mechanics, **14**(5), (2013), 414-423, DOI 10.1080/15502287.2013.784379.

26 **Falahatgar SR, Salehi M**, *Dynamic relaxation nonlinear viscoelastic analysis of annular sector composite plate*, Journal of Composite Materials, **43**(3), (2008), 257-275, DOI 10.1177/0021998308099221.

27 **Golmakani ME, Kadkhodayan M**, *Nonlinear bending analysis of annular FGM plates using higher-order shear deformation plate theories*, Composite Structures, **93**(2), (2011), 973-982, DOI 10.1016/j.compstruct.2010.06.024.

28 **Falahatgar SR, Salehi M**, *Nonlinear viscoelastic response of unidirectional polymeric laminated composite plates under bending loads*, Applied Composite Materials, **18**(6), (2011), 471-483, DOI 10.1007/s10443-011-9212-0.

29 **Brew JS, Brotton DM**, *Nonlinear structural analysis by dynamic relaxation*, International Journal for Numerical Methods in Engineering, **3**(4), (1971), 463-483, DOI 10.1002/nme.1620030403.

30 **Bunce JW**, *A note on the estimation of critical damping in dynamic relaxation*, International Journal for Numerical Methods in Engineering, **4**(2), (1972), 301-303, DOI 10.1002/nme.1620040214.

31 **Cassell AC, Hobbs RE**, *Numerical stability of dynamic relaxation analysis of non-linear structures*, International Journal for Numerical Methods in Engineering, **10**(6), (1976), 1407-1410, DOI 10.1002/nme.1620100620.

32 **Papadrakakis M**, *A method for the automatic evaluation of the dynamic relaxation parameters*, Computer Methods in Applied Mechanics and Engineering, **25**(1), (1981), 35-48, DOI 10.1016/0045-7825(81)90066-9.

33 **Underwood P**, *Dynamic relaxation(in structural transient analysis)*, Computational methods for transient analysis(A 84-29160 12-64). Amsterdam, North-Holland, (1983), 245-265.

34 **Qiang S**, *An adaptive dynamic relaxation method for nonlinear problems*, Computers & Structures, **30**(4), (1988), 855-859, DOI 10.1016/0045-7949(88)90117-4.

35 **Zhang LC, Kadkhodayan M, Mai YW**, *Development of the maDR method*, Computers & Structures, **52**(1), (1994), 1-8, DOI 10.1016/0045-7949(94)90249-6.

36 **Munjiza A**, *A Km proportional damping for dynamic relaxation*, International Journal for Engineering Modelling, **9**(1-4), (1996), 1-9.

37 **Munjiza A, Owen DRJ, Crook AJL**, *An M(M-1K)m proportional damping in explicit integration of dynamic structural systems*, International Journal for Numerical Methods in Engineering, **41**(7), (1998), 1277-1296, DOI 10.1002/(SICI)1097-0207(19980415)41:7<1277::AID-NME335>3.0.CO;2-9.

38 **Rezaiee-Pajand M, Taghavian Hakkak M**, *Nonlinear analysis of truss structures using dynamic relaxation*, International Journal of Engineering, **19**(1), (2006), 11-22.

39 **Kadkhodayan M, Alamatian J, Turvey GJ**, *A new fictitious time for the dynamic relaxation (DXDR) method*, International Journal for Numerical Methods in Engineering, **74**(6), (2008), 996-1018, DOI 10.1002/nme.2201.

40 **Rezaiee-Pajand M, Sarafrazi SR**, *Nonlinear structural analysis using dynamic relaxation method with improved convergence rate*, international Journal of Computational Methods, **7**(4), (2010), 627-654.

41 **Rezaiee-Pajand M, Alamatian J**, *The dynamic relaxation method using new formulation for fictitious mass and damping*, Structural Engineering and Mechanics, **34**(1), (2010), 109-133.

42 **Rezaiee-Pajand M, Kadkhodayan M, Alamatian J, Zhang LC**, *A new method of fictitious viscous damping determination for the dynamic relaxation method*, Computers & Structures, **89**(9 – 10), (2011), 783-794, DOI 10.1016/j.compstruc.2011.02.002.

43 **Rezaiee-Pajand M, Sarafrazi SR**, *Nonlinear dynamic structural analysis using dynamic relaxation with zero damping*, Computers & Structures, **89**(13 – 14), (2011), 1274-1285, DOI 10.1016/j.compstruc.2011.04.005.

44 **Rezaiee-Pajand M, Kadkhodayan M, Alamatian J**, *Timestep selection for dynamic relaxation method*, Mechanics Based Design of Structures and Machines, **40**(1), (2012), 42-72, DOI 10.1080/15397734.2011.599311.

45 **Alamatian J**, *A new formulation for fictitious mass of the Dynamic Relaxation method with kinetic damping*, Computers & Structures, **90 – 91**, (2012), 42-54, DOI 10.1016/j.compstruc.2011.10.010.

46 **Rezaiee-Pajand M, Sarafrazi SR, Rezaiee H**, *Efficiency of dynamic relaxation methods in nonlinear analysis of truss and frame structures*, Computers & Structures, **112 – 113**(0), (2012), 295-310, DOI 10.1016/j.compstruc.2012.08.007.

47 **Rezaiee-Pajand M, Rezaee H**, *Fictitious time step for the kinetic dynamic relaxation method*, Mechanics of Advanced Materials and Structures, **21**(8), (2012), 631-644, DOI 10.1080/15376494.2012.699603.

48 **Rezaiee H**, *Nonlinear structural analysis using dynamic relaxation method*, Master's thesis, Ferdowsi University; Mashhad, Iran, 2012. (In Persian).

49 **Topping BHV, Ivanyi P**, *Dynamic relaxation*, In: Computer aided design of cable membrane structures, Saxe-Coburg Publications; Scotland, 2008, pp. 39-84.

50 **Barnes MR**, *Form and stress engineering of tension structures*, Structural Engineering Review, **6**(3), (1994), 175-202.

51 **Rajasekaran S**, *Chapter 11*, In: Numerical solution methods for natural frequencies and mode shapes in relation to structural dynamics during earthquakes, Elsevier Science, 2009.